J|A|C|S ARTICLES

Published on Web 03/23/2010

Cobalt(II) "Scorpionate" Complexes as Models for Cobalt-Substituted Zinc Enzymes: Electronic Structure Investigation by High-Frequency and -Field Electron Paramagnetic Resonance Spectroscopy

J. Krzystek,[†] Dale C. Swenson,[‡] S. A. Zvyagin,[§] Dmitry Smirnov,[†] Andrew Ozarowski,[†] and Joshua Telser*,[||]

National High Magnetic Field Laboratory, Florida State University, Tallahassee, Florida 32310, Department of Chemistry, University of Iowa, Iowa City, Iowa 52242, Dresden High Magnetic Field Laboratory (HLD), Forschungszentrum Dresden-Rossendorf, D-01314 Dresden, Germany, and Department of Biological, Chemical and Physical Sciences, Roosevelt University, Chicago, Illinois 60605

Received December 30, 2009; E-mail: jtelser@roosevelt.edu

Abstract: A series of complexes of formula $Tp^{R,R'}CoL$, where $Tp^{R,R'-}$ = hydrotris(3-R,5-R′-pyrazol-1-yl)borate ("scorpionate") anion (R = *tert*-butyl, R′ = H, Me, 2′-thienyl (Tn), L = Cl^-, NCS^-, NCO^-, N_3^-), has been characterized by electronic absorption spectroscopy in the visible and near-infrared (near-IR) region and by high-frequency and -field electron paramagnetic resonance (HFEPR). Reported here are also crystal structures of seven members of the series that have not been reported previously: R′ = H, L = NCO^-, N_3^-; R′ = Me, L = Cl^-, NCS^-, NCO^-, N_3^-; R′ = Tn, L = Cl^-, NCS^-. These include a structure for $Tp^{tBu,Me}CoCl$ different from that previously reported. All of the investigated complexes contain a four-coordinate cobalt(II) ion ($3d^7$) with approximate C_{3v} point group symmetry about the metal ion and exhibit an $S = {}^3/_2$ high-spin ground state. The use of HFEPR allows extraction of the full set of *intrinsic* $S = {}^3/_2$ spin Hamiltonian parameters (*D*, *E*, and *g* values). The axial zero-field splitting parameter, *D*, for all investigated $Tp^{R,R'}CoL$ complexes is always positive, a fact not easily determined by other methods. However, the magnitude of this parameter varies widely: 2.4 $cm^{-1} \leq D \leq 12.7$ cm^{-1}, indicating the extreme sensitivity of this parameter to environment. The spin Hamiltonian parameters are combined with estimates of 3d energy levels based on the visible−near-IR spectra to yield ligand-field parameters for these complexes following the angular overlap model (AOM). This description of electronic structure and bonding in pseudotetrahedral cobalt(II) complexes can enhance the understanding of similar sites in metalloproteins, specifically cobalt-substituted zinc enzymes.

Introduction

The hydro(tris-pyrazol-1-yl)borate "scorpionate" anion has proven to be a popular and versatile ligand, binding to a wide variety of transition-metal ions in the 40 years since its synthesis by Trofimenko.[1−3] In addition to variation of the coordinated metal ion, variation of substituents on the pyrazole rings allows for the synthesis of a large number of related scorpionate complexes. The steric and electronic effects of these substituents on the geometrical and electronic structure of the metal ion can then be probed.

Our interest in scorpionate complexes is based on the above general factors and on several specific points of coordination chemistry. With the appropriate substituents, the monoanionic, tridentate scorpionate ligand (Tp^-) supports four-coordinate complexes of general formula TpML. For M^{2+} and L = monoanionic ligands such as halides and pseudohalides, a neutral complex results. Such a complex can be readily studied in noncoordinating organic solvents and is absent the complication of interionic forces in the solid state. More importantly, the scorpionate geometry supports TpML complexes of pseudotetrahedral, idealized C_{3v} point group symmetry, and thus for appropriate paramagnetic ions, a high-spin (HS) electronic ground state results, in contrast to low-spin (LS) ground states in, for example, square-planar complexes.

The specific metal ion studied here is Co(II) ($3d^7$, $S = {}^3/_2$). Complexes of general type TpCoL are of inherent interest in terms of understanding the electronic structure of HS Co(II) complexes as a function of coordination environment. HS Co(II) complexes themselves are of specific, biological interest as models for the active sites of many metalloproteins. In particular, Co(II) substitution has been widely employed as a tool for conversion of "spectroscopically silent" Zn(II)-containing proteins into still-functioning enzymes, but for which optical (absorption, magnetic circular dichroism (MCD)) and magnetic resonance (nuclear magnetic resonance (NMR), electron para-

[†] Florida State University.
[‡] University of Iowa.
[§] Forschungszentrum Dresden-Rossendorf.
[||] Roosevelt University.

(1) Trofimenko, S. *J. Am. Chem. Soc.* **1967**, *89*, 6288–6294.
(2) Trofimenko, S., *Scorpionates: The Coordination Chemistry of Polypyrazolylborate Ligands*; Imperial College Press: London, 1999; p 292.
(3) Trofimenko, S. *Polyhedron* **2004**, *23*, 197–203.

magnetic resonance (EPR), electron nuclear double resonance (ENDOR)) spectroscopic techniques all can be productively applied to understand enzyme structure and function.[4−6] Recent examples involved EPR/ENDOR studies of a Co-substituted Zn-finger protein, TF IIIA,[7] and MCD studies of a variety of Co-substituted Zn enzymes and model compounds.[8,9] Scorpionate complexes of both Zn(II) and Co(II) have been promoted as models for Zn enzymes, such as carbonic anhydrase.[10] In particular, the N3 donor set of the scorpionate ligand mimics the tris-histidine motif found in many zinc metalloenzymes.[11] Pentacoordinate Co(II) scorpionates have been used as structural and spectroscopic (EPR, NMR) models for Zn matrix metalloproteinases.[12] Thus, an improved understanding of the electronic structure of Co(II) in TpCoL complexes could enhance our understanding of relevant properties of a wide range of metalloproteins.

HS Co(II) was the subject of an earlier high-frequency and -field EPR (HFEPR) study by some of us, in the complex $CoCl_2(PPh_3)_2$: a four-coordinate, pseudotetrahedral complex of idealized C_{2v} symmetry.[13] In the present study, we describe a HFEPR investigation of a series of idealized C_{3v} symmetry scorpionate complexes of Co(II), of general formula $Tp^{R,R'}CoL$, where $Tp^{R,R'}$ = hydrotris(3-R,5-R′-pyrazol-1-yl)borate anion (R = *tert*-butyl (*t*-Bu), R′ = H, Me, 2′-thienyl (Tn), L = Cl^-, NCS^-, NCO^-, N_3^-). The 3-substituent, R = *t*-Bu, is necessary to prevent formation of six-coordinate bis-scorpionate complexes, Tp_2Co, which are of interest in their own right.[14] The 5-substituents, R′ = H, Me, Tn, were chosen to span a range of steric requirements, ranging from hydrogen and the minimally bulky methyl group to the very bulky and π-interacting 2′-thienyl group. The axial ligand, L, represents a standard series of pseudohalogens that are all N-donors, along with chloride, the halogen that forms the only extensive series of $Tp^{R,R'}CoL$ complexes. The complexes all have either an N4 donor set or N3Cl.

The electronic structure of paramagnetic transition-metal complexes can be fruitfully studied by EPR;[15] however, this technique can be fraught with difficulty when systems with $S > {}^1/_2$ are investigated, because of an often large zero-field splitting (zfs) characterizing such complexes. For HS Co(II) specifically, conventional (X- or Q-band) EPR data can be only analyzed in terms of an effective $S = {}^1/_2$ spin Hamiltonian, yielding little information on the *intrinsic* parameters of the $S = {}^3/_2$ state. However, over the past few years, HFEPR has been shown to be extremely useful in studying such systems and extracting accurate and precise spin Hamiltonian parameters from them[16] and is thus the principal experimental technique behind this work.

Electronic absorption spectroscopy over the UV−visible−near-IR range was also applied to the complexes studied here and provides important information on electronic structure. As the crystal structures of only two complexes, $Tp^{t\text{-Bu,H}}CoL$ with L = Cl^-, NCS^-, had been previously reported respectively by Gorrell and Parkin and by Trofimenko et al.,[17,18] the crystal and molecular structures of the remaining eight of these ($Tp^{t\text{-Bu,H}}CoL$ (L = NCO^-, N_3^-), $Tp^{t\text{-Bu,Me}}CoL$ (L = Cl^-, NCS^-, NCO^-, N_3^-), $Tp^{t\text{-Bu,Tn}}CoL$ (L = Cl^-, NCS^-)) were determined. During the course of this study, the structure of $Tp^{t\text{-Bu,Me}}CoCl$ was reported;[19] however, it differs from that determined here. The complexes $Tp^{t\text{-Bu,Tn}}CoL$ (L = NCO^-, N_3^-) did not yield HFEPR spectra suitable for analysis; thus, their structures were not determined.

Experimental Section

Materials. The complexes $Tp^{R,R'}CoL$ (R = 3-*t*-Bu, R′ = 5-(H, Me, Tn (2′-thienyl)), L = Cl^-, NCS^-, NCO^-, N_3^-) were a gift of the late Dr. S. Trofimenko, University of Delaware. The synthesis of these and related complexes has been described in general elsewhere.[2,3] Specifically, $Tp^{t\text{-Bu,H}}$ and its metal complexes were prepared as described by Trofimenko et al. in 1987[18] and $Tp^{t\text{-Bu,Me}}$ and its metal complexes by Trofimenko et al. in 1992.[20] For $Tp^{t\text{-Bu,Tn}}$, the procedure given by Calabrese et al.[21] was used, but with ethyl pivalate rather than ethyl formate to yield the *t*-Bu-substituted product.

X-ray Crystallography. Single crystals of $Tp^{t\text{-Bu,R'}}CoL$ (R′ = H, L = NCO^-, N_3^-; R′ = Me, L = Cl^-, NCS^-; R′ = 2′-thienyl (Tn), L = Cl^-, NCS^-) were each grown from dichloromethane solution that was layered with hexanes. In the cases of $Tp^{t\text{-Bu,Me}}CoL$ (L = NCO^-, N_3^-), this procedure led to twinned crystals. However, in these two complexes, crystals suitable for structure determination were grown by slow evaporation of toluene solutions. The structure determination for each is given below.

$Tp^{t\text{-Bu,H}}Co(NCO)$. A green-blue plate (0.22 × 0.20 × 0.02 mm) of $Tp^{t\text{-Bu,H}}Co(NCO)$ was isolated from the sample and mounted with grease on the tip of a glass capillary epoxied to a brass pin and placed on the diffractometer with the long crystal dimension (unit cell *c* axis) approximately parallel to the diffractometer ϕ axis. Data were collected on a Nonius KappaCCD diffractometer (Mo Kα radiation, graphite monochromator) at 190(2) K (cold N_2 gas stream) using standard CCD techniques, yielding 41 469 data.[22] Lorentz and polarization corrections were applied. A correction for absorption using the multiscan technique was applied (T_{max} = 0.9862, T_{min} = 0.8622). Equivalent data were averaged yielding 5874 unique data (R_{int} = 0.089, 3610 $F > 4[\sigma(F)]$). On the basis of a preliminary examination of the crystal, the space group $P2_1/n$ was assigned (no exceptions to the systematic absences: $h0l$ with $h + l$ = odd and $0k0$ with k = odd were noted). The computer programs from the

(4) Maret, W.; Vallee, B. L. *Methods Enzymol.* **1993**, *226*, 52–71.
(5) Bertini, I.; Luchinat, C.; Piccioli, M. *Methods Enzymol.* **2001**, *339*, 314–40.
(6) Bertini, I.; Luchinat, C.; Parigi, G., *Solution NMR of Paramagnetic Molecules: Applications to Metallobiomolecules and Models*; Elsevier Science: Amsterdam, 2001; Vol. 2.
(7) Walsby, C. J.; Krepkiy, D.; Petering, D. H.; Hoffman, B. M. *J. Am. Chem. Soc.* **2003**, *125*, 7502–7503.
(8) Werth, M. T.; Tang, S.-F.; Formicka, G.; Zeppezauer, M.; Johnson, M. K. *Inorg. Chem.* **1995**, *34*, 218–228.
(9) Larrabee, J. A.; Alessi, C. M.; Asiedu, E. T.; Cook, J. O.; Hoerning, K. R.; Klingler, L. J.; Okin, G. S.; Santee, S. G.; Volkert, T. L. *J. Am. Chem. Soc.* **1997**, *119*, 4182–4196.
(10) Bergquist, C.; Fillebeen, T.; Morlok, M. M.; Parkin, G. *J. Am. Chem. Soc.* **2003**, *125*, 6189–6199.
(11) Parkin, G. *Chem. Rev.* **2004**, *104*, 699–768.
(12) Jacobsen, F. E.; Breece, R. M.; Myers, W. K.; Tierney, D. L.; Cohen, S. M. *Inorg. Chem.* **2006**, *45*, 7306–7315.
(13) Krzystek, J.; Zvyagin, S. A.; Ozarowski, A.; Fiedler, A. T.; Brunold, T. C.; Telser, J. *J. Am. Chem. Soc.* **2004**, *126*, 2148–2155.
(14) Myers, W. K.; Duesler, E. N.; Tierney, D. L. *Inorg. Chem.* **2008**, *47*, 6701–6710.
(15) Abragam, A.; Bleaney, B., *Electron Paramagnetic Resonance of Transition Ions*; Dover Publications: New York, 1986.
(16) Krzystek, J.; Ozarowski, A.; Telser, J. *Coord. Chem. Rev.* **2006**, *250*, 2308–2324.
(17) Gorrell, I. B.; Parkin, G. *Inorg. Chem.* **1990**, *29*, 2452–2456.
(18) Trofimenko, S.; Calabrese, J. C.; Thompson, J. S. *Inorg. Chem.* **1987**, *26*, 1507–1514.
(19) Ferrence, G. M.; Beitelman, A. D. *Acta Crystallogr.* **2007**, *E63*, m153–m155.
(20) Trofimenko, S.; Calabrese, J. C.; Kochi, J. K.; Wołowiec, S.; Hulsbergen, F. B.; Reedijk, J. *Inorg. Chem.* **1992**, *31*, 3943–3950.
(21) Calabrese, J. C.; Domaille, P. J.; Trofimenko, S.; Long, G. J. *Inorg. Chem.* **1991**, *30*, 2795–2801.
(22) Collect, Nonius BV, Delft, The Netherlands, 1997−2000.

HKL package were used for data reduction.[23,24] The preliminary model of the structure was obtained using XS, a direct methods program. Least-squares refinement of the model vs the data was performed with the XL computer program. Both are in the SHELXTL v6.1 package.[25] All non-hydrogen atoms were refined with anisotropic thermal parameters. All H atoms were included with the riding model using the XL program default values. No further restraints or constraints were imposed on the refinement model.

Tp$^{t\text{-Bu,H}}$CoN$_3$. The same procedure as described above for Tp$^{t\text{-Bu,H}}$Co(NCO) was used on a blue prism (0.25 × 0.21 × 0.14 mm) of Tp$^{t\text{-Bu,H}}$CoN$_3$ with the long crystal dimension (unit cell *b* axis) approximately parallel to the diffractometer ϕ axis, and 53 457 data were collected. A correction for absorption was applied (T_{max} = 0.9084, T_{min} = 0.8446). Equivalent data were averaged, yielding 5840 unique data (R_{int} = 0.033, 4806 $F > 4[\sigma(F)]$). The space group $P2_1/n$ was assigned as described above. Refinement was as described above.

Tp$^{t\text{-Bu,Me}}$CoCl. The same procedure as described above for Tp$^{t\text{-Bu,H}}$Co(NCO) was used on a blue needle (0.30 × 0.06 × 0.05 mm) of Tp$^{t\text{-Bu,Me}}$CoCl with the long crystal dimension (unit cell *ab* diagonal) approximately parallel to the diffractometer ϕ axis, and 9505 data were collected. A correction for absorption was applied (T_{max} = 0.964, T_{min} = 0.810). Equivalent data were averaged, yielding 1175 unique data (R_{int} = 0.035, 1148 $F > 4[\sigma(F)]$). The space group *R*3*m* was assigned as described above (no exceptions to the systematic absences were noted). The molecule resides on a crystallographic 3*m* site. The structure is an inversion twin (fraction 0.442(0.015)). The methyl H atoms were disordered over two sites (related by a 60° rotation about the C−Me bond) with idealized geometry.

Tp$^{t\text{-Bu,Me}}$Co(NCS). The same procedure as described above for Tp$^{t\text{-Bu,H}}$Co(NCO) was used on a green-blue plate (0.33 × 0.27 × 0.03 mm) of Tp$^{t\text{-Bu,Me}}$Co(NCS) with the long crystal dimension (unit cell *a* axis) approximately parallel to the diffractometer ϕ axis, and 54 226 data were collected. A correction for absorption was applied (T_{max} = 0.984, T_{min} = 0.809). Equivalent data were averaged, yielding 6838 unique data (R_{int} = 0.079, 4399 $F > 4[\sigma(F)]$). The space group $P2_1/n$ was assigned as described above. Refinement was as described above.

Tp$^{t\text{-Bu,Me}}$Co(NCO). The same procedure as described above for Tp$^{t\text{-Bu,H}}$Co(NCO) was used on a blue plate (0.38 × 0.22 × 0.05 mm) of Tp$^{t\text{-Bu,Me}}$Co(NCO) with the long crystal dimension (unit cell *c* axis) approximately parallel to the diffractometer ϕ axis, and 59 524 data were collected. A correction for absorption was applied (T_{max} = 0.966, T_{min} = 0.790). Equivalent data were averaged, yielding 6790 unique data (R_{int} = 0.051, 4684 $F > 4[\sigma(F)]$). The space group $P2_1/n$ was assigned as described above. The C12−C15 *t*-Bu group was rotationally (~60° about the C9−C12 bond) disordered (occupancy: C13, C14, C15, 0.918(4); C13′, C14′, C15′, 0.082(4)). The conformations of the disordered *t*-Bu groups were restrained to be the same. C13′, C14′, and C15′ were assigned a single isotropic displacement parameter. No further restraints or constraints were imposed on the refinement model.

Tp$^{t\text{-Bu,Me}}$CoN$_3$. The same procedure as described above for Tp$^{t\text{-Bu,H}}$Co(NCO) was used on a blue plate (0.33 × 0.19 × 0.01 mm) of Tp$^{t\text{-Bu,Me}}$CoN$_3$ with the long crystal dimension (unit cell *ac* diagonal) approximately parallel to the diffractometer ϕ axis, and 48 065 data were collected. A correction for absorption using the multiscan technique was applied (T_{max} = 0.994, T_{min} = 0.833). Equivalent data were averaged, yielding 5569 unique data (R_{int} = 0.054, 4229 $F > 4[\sigma(F)]$). The space group $P2_1/n$ was assigned as described above. The azide ligand was disordered over two orientations (relative occupancies 0.77(1):0.23(1)). The conformations were restrained to be the same with matching displacement parameters. A molecule of toluene solvent was included near an inversion center. It is disordered and was modeled with idealized rigid groups (occupancies 0.22, 0.11, and 0.17, respectively, for the C10*, C20*, and C30* groups). Each group had an overall isotropic displacement parameter. No further restraints or constraints were imposed on the refinement model.

Tp$^{t\text{-Bu,Tn}}$CoCl. The same procedure as described above for Tp$^{t\text{-Bu,H}}$Co(NCO) was used on a blue needle (0.38 × 0.04 × 0.04 mm) of Tp$^{t\text{-Bu,Tn}}$CoCl with the long crystal dimension (unit cell *b* axis) approximately parallel to the diffractometer ϕ axis, and 68 370 data were collected. A correction for absorption was applied (T_{max} = 0.9722, T_{min} = 0.7485). Equivalent data were averaged, yielding 7128 unique data (R_{int} = 0.070, 4920 $F > 4[\sigma(F)]$). The space group *C*2/*c* was assigned (no exceptions to the systematic absences: *hkl* with $h + k$ = odd and *h*0*l* with l = odd were noted). Refinement was as described above.

Two molecules of CH_2Cl_2 solvent were located near symmetry elements and found to have high thermal motion. Each was modeled as two disordered rigid groups (C−Cl = 1.75 Å, C−H = 0.99 Å, tetrahedral angles) of equal occupancy with a single isotropic thermal parameter. The net occupancy at each site is 0.5. The 2-thienyl substituent (C28, S29, C30, C31, C32) was found to be disordered over two orientations (180° rotation about the C9−C28 bond). The relative occupancy was refined to 0.656:0.344(5). Atoms in close proximity were given the same anisotropic thermal parameters (i.e., U_{aniso}(C28) = U_{aniso}(C28′), U_{aniso}(S29) = U_{aniso}(C32′), etc.). The minor orientation (primed labels) was restrained to have the same conformation as the major orientation, and both were restrained to be flat.

Tp$^{t\text{-Bu,Tn}}$Co(NCS). The same procedure as described above for Tp$^{t\text{-Bu,H}}$Co(NCO) was used on a blue plate (0.19 × 0.13 × 0.06 mm) of Tp$^{t\text{-Bu,Tn}}$Co(NCS) with the long crystal dimension (unit cell *c* axis) approximately parallel to the diffractometer ϕ axis, and 54 745 data were collected. A correction for absorption was applied (T_{max} = 0.9586, T_{min} = 0.8767). Equivalent data were averaged, yielding 8614 unique data (R_{int} = 0.052, 6123 $F > 4[\sigma(F)]$). The space group $P2_1/c$ was assigned (no exceptions to the systematic absences: *h*0*l* with l = odd and 0*k*0 with k = odd were noted). Refinement was as described above.

Late difference maps suggested disorder in the NCS$^-$ ligand, which was refined as such. The relative occupancy was refined to 0.945(3):0.055(3). The minor site was restrained to have the same conformation, with the N atoms occupying the same site and U_{iso}(C1′) = $U_{iso,eq}$(C1) and U_{iso}(S1′) = $U_{iso,eq}$(S1). The C28−C32 and C33−C37 2′-thienyl groups were each disordered via 2-fold rotation about the C9−C28 and C16−C33 bonds, respectively. The disorder pairs were restrained to have the same conformations. Atoms occupying the same relative site (e.g., S29, C32′; C30, C31′; C31, C3′; C32, S29′; etc.) were constrained to have the same anisotropic thermal parameters. The relative occupancies were refined to 0.609:0.396(3) for the C28−C32 2′-thienyl group and 0.869:0.131(3) for the C33−C37 2-thienyl group.

Electronic Absorption Spectroscopy. Ultraviolet−visible−near-infrared (UV−vis−near-IR) spectra were recorded for samples of the respective Tp$^{t\text{-Bu,R}'}$CoL (L = Cl$^-$, NCS$^-$, NCO$^-$, N$_3^-$) complexes dissolved in carbon tetrachloride using a Jasco 570 spectrophotometer with samples in 1 cm path length Suprasil cuvettes over the range 25 000−4000 cm^{-1} (400−2500 nm) at ambient temperature. Carbon tetrachloride was chosen as an inert solvent that is absent C−H stretching overtones which can complicate the near-IR region. All of the Tp$^{t\text{-Bu,R}'}$CoL complexes are sufficiently soluble in CCl_4 (>0.1 mM) to provide satisfactory UV−vis−near-IR spectra.

Infrared Spectroscopy. Infrared (IR) spectra were recorded for Tp$^{t\text{-Bu,Tn}}$CoL L = Cl$^-$, NCS$^-$, using a Thermo IR200 spectrophotometer with samples as Nujol mulls. IR spectra were also recorded in 0.1 mm path length solution cells for CH_2Cl_2 solutions of Tp$^{t\text{-Bu,Tn}}$CoCl in an attempt to observe low-energy ligand field

(23) Otwinowski, Z.; Minor, V. Macromolecular Crystallography, Part A. In *Methods in Enzymoology*, Carter, C., Jr., Sweet, R. M., Eds.; Academic Press: New York, 1997; Vol. 26, pp 307−326.
(24) Otwinowski, Z.; Minor, V. HKL Scalepack, 1997.
(25) Sheldrick, G. M. SHELXTL, 6.1; Bruker AXS Inc., Madison, WI, 2001.

transitions (~3000−4000 cm^{-1}; see Discussion). Comparison with neat solvent gave no clear evidence for bands other than vibrational bands. Carbon tetrachloride, used for the UV−vis−near-IR spectra, would have been preferable as a solvent for IR, but even $Tp^{t\text{-}Bu,Tn}CoCl$, which was selected for its higher solubility relative to the $Tp^{t\text{-}Bu,H}CoL$ complexes, was not sufficiently soluble in CCl_4 to be useful for IR investigation.

HFEPR Spectroscopy. HFEPR spectra were recorded using primarily the Millimeter and Submillimeter Wave Facility at NHMFL,[26] with additional experiments performed at the EMR Facility.[27] The former experimental setup currently employs tunable frequencies achieved with backward wave oscillator (BWO) sources in the 70−900 GHz range, of which 120−700 GHz was available in the present study, and the resistive "Keck" magnet enabling 0−25 T field sweeps. The latter facility uses a variety of solid-state sources in conjunction with a 15/17 T superconducting magnet. Detection was provided with an InSb hot-electron bolometer (QMC Ltd., Cardiff, U.K.). Modulation for detection purposes was provided alternatively by chopping the sub-THz wave beam ("optical modulation") or by modulating the magnetic field. The relative merits of both types of modulation were discussed in a previous paper by some of us.[28] A Stanford Research Systems SR830 lock-in amplifier converted the modulated signal to dc voltage.

Typically, 30−50 mg of ground solid polycrystalline sample was used for HFEPR. In previous HFEPR studies of magnetically nondiluted paramagnetic solids, torquing (i.e., magnetic field-induced alignment) of microcrystallites occurred.[29] In this work, such effects were generally not observed, an exception being $Tp^{t\text{-}Bu,H}CoN_3$, which was thus investigated both as a loose powder and by immobilization in a KBr pellet. Two complexes of the $Tp^{t\text{-}Bu,Tn}CoL$ series, $L = NCO^-$, N_3^-, were very fluffy rather than microcrystalline. As a result, it was not possible to grind them or load the sample container with sufficient amount to obtain satisfactory spectra.

EPR Analysis. The magnetic properties of an ion with $S = {}^3/_2$ can be described by the standard spin Hamiltonian comprised of Zeeman and second-rank zfs terms:[15]

$$\mathscr{H} = \beta B \cdot \mathbf{g} \cdot S + D(S_z^2 - S(S+1)/3) + E(S_x^2 - S_y^2) \qquad (1)$$

For $S = {}^3/_2$, higher order Zeeman interactions may be present,[30] but these were not considered here. In zero field, the $|S, M_S\rangle = |{}^3/_2, \pm{}^3/_2\rangle$ and $|{}^3/_2, \pm{}^1/_2\rangle$ Kramers spin doublets are separated by the energy gap (often called "zero-field splitting" in the literature) $\Delta = |2D\{1 + 3(E/D)^2\}^{1/2}| \approx 2|D|$ for small E. Field-swept HFEPR provides turning points in a powder pattern; their 2-D frequency vs field dependencies (maps) were fitted by use of a nonlinear least-squares procedure that we have employed previously for Co(II).[13] Further details of the tunable-frequency EPR methodology are given elsewhere.[28]

Ligand-Field Theory (LFT) Analysis. LFT analysis of the electronic structure of Co(II) in $Tp^{t\text{-}Bu,R'}CoL$ complexes was performed with use of the angular overlap model (AOM).[31] Two computer programs were employed, Ligfield, written by J. Bendix (Ørsted Institute, Copenhagen, Denmark),[32] and a locally written program, DDN, which is available from J. Telser. Both programs use the complete d^7 (equivalent to d^3) weak-field basis set including interelectronic repulsion (Racah parameters: B, C), spin−orbit coupling (SOC constant: ζ),[32] and AOM ligand-field bonding parameters (ϵ_σ, ϵ_π) and gave identical results when directly compared. DDN allows use of a nonlinear least-squares fitting subroutine (DSTEPIT, from QCPE, Bloomington, IN) to match observed electronic transition energies to those calculated by user-defined variable parameters such as B, ϵ_σ, etc. The general AOM procedure involved an initial fit of spin-allowed optical transitions with variation of Racah B and AOM bonding parameters and with $\zeta \equiv 0$ (and C very large). To make the fitting tractable, the bonding parameters for the three pyrazole N donors were held identical (i.e., imposed C_3 bonding symmetry). From this initial fit, ζ was systematically varied (along with $C \equiv 4.7B$) until a reasonable match was obtained for $|D|$ in relation to experimental values. The resulting electronic transitions were then checked to ensure that they were still in agreement with experiment; if not, then the AOM parameters were adjusted to correct discrepancies. DDN also allows inclusion of an external magnetic field to be applied along the molecular axes (defined by the AOM) to give Zeeman splitting of energy levels from which g values can be calculated, as described previously.[33] This calculation was done for complexes only where the zfs was well-modeled by the AOM parameters.

Results

X-ray Crystallography. Crystal, collection, and refinement parameters for $Tp^{t\text{-}Bu,H}CoL$ ($L = NCO^-$, N_3^-), $Tp^{t\text{-}Bu,Me}CoL$ ($L = Cl^-$, NCS^-, NCO^-, N_3^-), and $Tp^{t\text{-}Bu,Tn}CoL$ ($L = Cl^-$, NCS^-) are presented in Table S1, and molecular structures are shown in Figures S1−S8 (Supporting Information), respectively. Selected bond distances and angles for these complexes are presented in Table S2. Molecular structures of the two complexes of the $Tp^{t\text{-}Bu,H}$ ligand determined in this work are shown in Figure 1, together with the structures of $Tp^{t\text{-}Bu,H}CoL$ ($L = Cl^-$,[17] NCS^-),[18] so that the complete series of L can be seen for the simplest given set of substituents: R = *t*-Bu, R′ = H. For all of the complexes with the $Tp^{t\text{-}Bu,H}$ ligand, there are no solvent molecules or any disorder, nor is there any disorder for $Tp^{t\text{-}Bu,Me}CoCl$ or $Tp^{t\text{-}Bu,Me}Co(NCS)$. However, for several of the other complexes, there is disorder and/or solvent molecules of crystallization. For $Tp^{t\text{-}Bu,Me}Co(NCO)$, there is disorder in one of the *t*-Bu groups (see the Experimental Section), which is of little consequence. In $Tp^{t\text{-}Bu,Me}CoN_3$, however, which proved relatively difficult to crystallize, there is disorder in the azido ligand and there is a disordered molecule of toluene from solvent. For $Tp^{t\text{-}Bu,Tn}CoCl$, one disordered molecule of CH_2Cl_2, derived from solvent, was found per metal complex and was located in two sites of equal occupancy (see the Experimental Section). One of the two thienyl groups on each $Tp^{t\text{-}Bu,Tn}$ ligand is also slightly disordered. In the case of $Tp^{t\text{-}Bu,Tn}Co(NCS)$, both thienyl groups on each ligand are disordered, as is the thiocyanate ligand (see the Experimental Section). No prior examples of $Tp^{t\text{-}Bu,Tn}ML$ have been structurally characterized; however, six-coordinate $(Tp^{Tn,H})_2Co$ ($Tp^{Tn,H-}$ is hydrotris[3-(2′-thienyl)pyrazol-1-yl]borate) has been structurally characterized as both benzene and dichloromethane solvates, and in each case, there was evidence of 2-fold disorder of the thienyl rings,[21] similar to that seen here, resulting from facile rotation about the 3C−2′C bond (C11−C28, C18−C33). Structural comparisons among $Tp^{R,R'}CoL$ complexes are made in the Supporting Information. No attempts at crystal structure determination were

(26) Zvyagin, S. A.; Krzystek, J.; van Loosdrecht, P. H. M.; Dhalenne, G.; Revcolevschi, A. *Phys. B* **2004**, *1−5*, 346–347.
(27) Hassan, A. K.; Pardi, L. A.; Krzystek, J.; Sienkiewicz, A.; Goy, P.; Rohrer, M.; Brunel, L.-C. *J. Magn. Reson.* **2000**, *142*, 300–312.
(28) Krzystek, J.; Zvyagin, S. A.; Ozarowski, A.; Trofimenko, S.; Telser, J. *J. Magn. Reson.* **2006**, *178*, 174–183.
(29) Krzystek, J.; Telser, J.; Pardi, L. A.; Goldberg, D. P.; Hoffman, B. M.; Brunel, L.-C. *Inorg. Chem.* **1999**, *38*, 6121–6129.
(30) McGavin, D. G.; Tennant, W. C.; Weil, J. A. *J. Magn. Reson.* **1990**, *87*, 92–109.
(31) Figgis, B. N.; Hitchman, M. A. *Ligand Field Theory and its Applications*; Wiley-VCH: New York, 2000.
(32) Bendix, J.; Brorson, M.; Schäffer, C. E. *Inorg. Chem.* **1993**, *32*, 2838–2849.
(33) Krzystek, J.; Fiedler, A. T.; Sokol, J. J.; Ozarowski, A.; Zvyagin, S. A.; Brunold, T. C.; Long, J. R.; Brunel, L.-C.; Telser, J. *Inorg. Chem.* **2004**, *43*, 5645–5658.

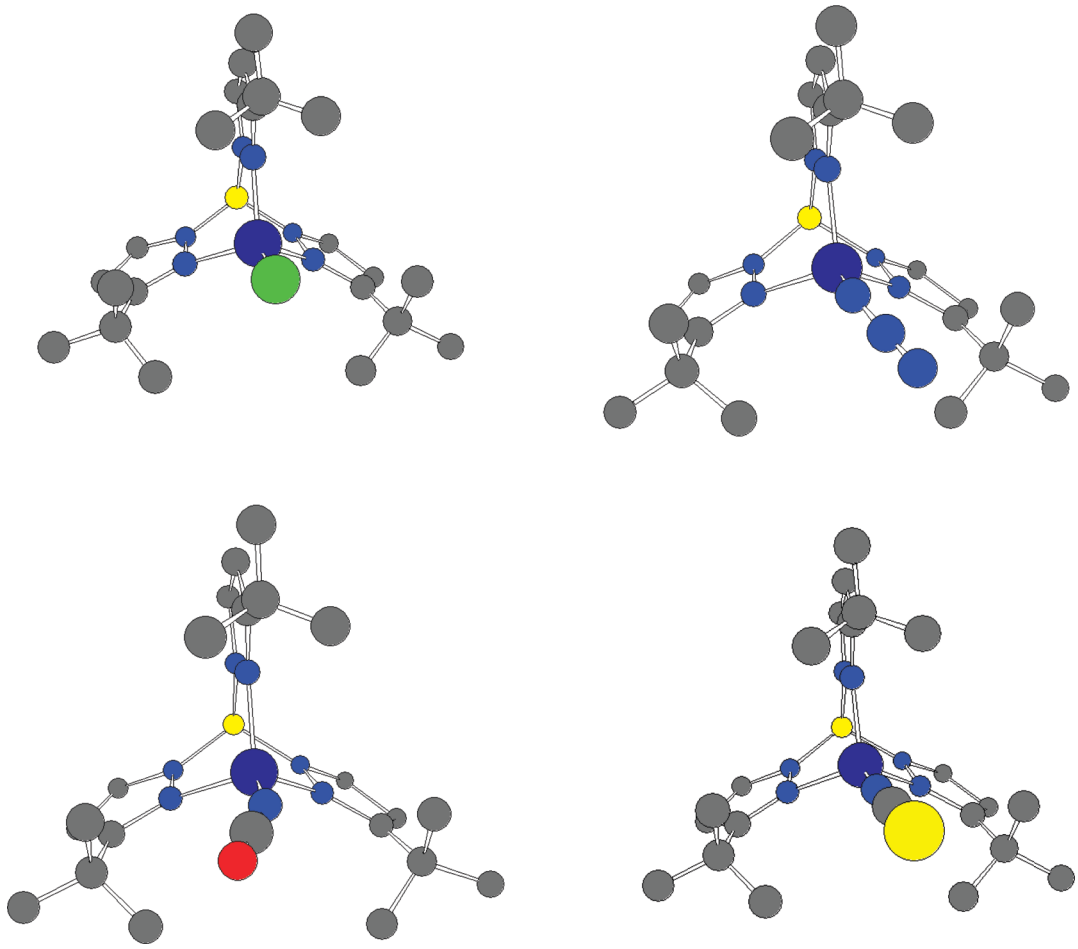

Figure 1. Molecular structures of $Tp^{t\text{-}Bu,H}CoL$: L = Cl^- (upper left), NCO^- (lower left), N_3^- (upper right), NCS^- (lower right). Complexes with L = NCO^-, N_3^- are from this work; those with L = Cl^-, NCS^- have been previously reported respectively by Gorrell and Parkin[17] and by Trofimenko et al.[18]

made for $Tp^{t\text{-}Bu,Tn}CoL$ (L = N_3^-, NCO^-), as these two complexes did not provide usable HFEPR spectra (see below).

Electronic Absorption Spectroscopy. UV−vis−near-IR spectra for entire series of complexes investigated by HFEPR, $Tp^{t\text{-}Bu,H}CoL$ (L = Cl^-, NCS^-, NCO^-, N_3^-), $Tp^{t\text{-}Bu,Me}CoL$ (L = Cl^-, NCS^-, NCO^-, N_3^-), and $Tp^{t\text{-}Bu,Tn}CoL$ (L = Cl^-, NCS^-), were recorded in CCl_4 solution over the range 25 000−4000 cm^{-1}. Electronic absorption data are summarized in detail in Table S3. As shown in Figure 2, all of the complexes exhibit qualitatively the same spectra when scaled to the same maximum band absorbance (at 15 000−16 000 cm^{-1}; 640−670 nm), which gives rise to the characteristic blue color of these and many other tetrahedral Co(II) complexes. This spectral similarity suggests very similar electronic structures for the Co(II) ion in all of these complexes. However, as given in Table S3 and shown graphically in Figure S9 (Supporting Information), the extinction coefficient of their absorbance varies by nearly an order of magnitude. The most strongly absorbing is the complex with an azido ligand (ϵ_{676} = 3520 M^{-1} cm^{-1}) and then the two complexes with thiocyanato ligands (ϵ_{645} = 1600−2400 M^{-1} cm^{-1}), while the two chloro complexes exhibit extinction coefficients in the range 400−700 M^{-1} cm^{-1}. The effect of the 5-(2′-thienyl) substituent on the vis−near-IR spectra is minimal, as is that of the 5-methyl group, as expected. Band assignments will be proposed in the Discussion.

HFEPR Spectroscopy. Results will be grouped by type of $Tp^{t\text{-}Bu,R'}$ ligand, beginning in more detail with the simplest ligand, R′ = H, followed by R′ = Me, and finally R′ = Tn, which is not complete in L. Within these groupings by scorpionate ligand, the results are discussed in order of axial ligand as follows: L = NCS^-, NCO^-, N_3^-, Cl^-. The chloro complexes were discussed first in X-ray Crystallography (e.g., Table 1), because Cl^- is structurally the simplest ligand. However, from the point of view of spectroscopy, this period 3 element is more complicated than the nitrogen donors and is thus discussed last in this section. Each complex except $Tp^{t\text{-}Bu,Tn}Co(NCO)$ and $Tp^{t\text{-}Bu,Tn}CoN_3$ produced strong spectra of well-defined shape, varying strongly between complexes within the same $Tp^{t\text{-}Bu,R'}CoL$ series, as shown in Figure 3 for the $Tp^{t\text{-}Bu,H}CoL$ series. The observed resonances could be divided into two groups: the intra-Kramers transitions, i.e., those corresponding to transitions within either the $M_S = \pm^1/_2$ or $\pm^3/_2$ doublet, and inter-Kramers ones, i.e. those occurring *between* the two Kramers doublets. The former extrapolate to zero frequency with field decreasing to zero, while the latter converge at some finite frequency value in zero field. The approximate value of the zero-field gap Δ was read directly from the 2-D field/frequency map of resonances (Figure 4 and Figures S10 and S11 in the Supporting Information) for the given complex, while accurate values of both second-rank zfs parameters and the values of the **g** matrix were obtained by a computer best fit of that map. The sign of D was obtained from simulating single-frequency spectra (two of those spectra are shown in Figure 5) and was found to be positive for all complexes. The parameter E was

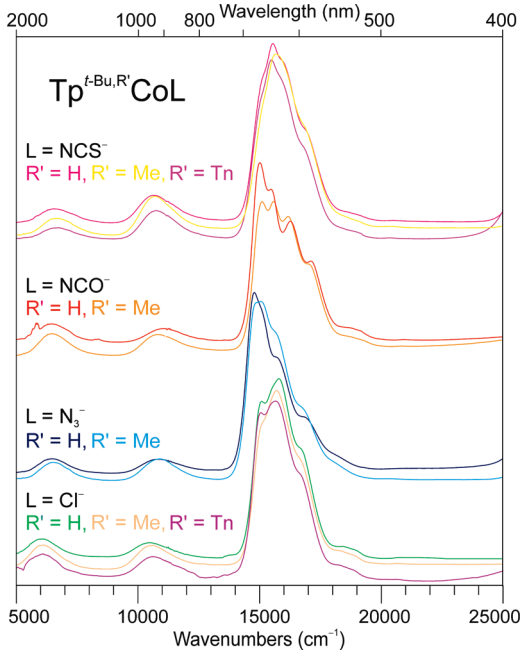

Figure 2. Electronic absorption spectra for $Tp^{R,R'}CoL$ (R = *t*-Bu, R′ = H, Me, Tn; L = NCS^-, NCO^-, N_3^-, Cl^-) complexes in CCl_4 solution at room temperature. The specific complexes are identified by the color of the trace, as indicated on the figure, and are grouped by L. The spectra have been arbitrarily scaled so that the maximum absorbance is the same in all cases to highlight the qualitatively similar appearance of the spectral series. Spectra with a quantitative ordinate in molar absorptivity are shown in Figure S9 (Supporting Information).

ascribed the same positive value by convention. This determination of the sign of *D* is an achievement of HFEPR that is difficult to match by other techniques such as magnetometry and MCD.[13,34] The refined set of the spin Hamiltonian parameters for each complex is given in Table 3, which also includes the resulting experimental values for Δ and those calculated by LFT (see below).

$Tp^{t\text{-}Bu,H}$CoL Series. All complexes in this series produced well-defined resonances, although those for the NCS^- complex were quite broad.

$Tp^{t\text{-}Bu,H}$Co(NCS). The 2-D field/frequency map is shown in Figure 4a, which demonstrates that all the turning points observed in the available frequency region correspond to the situation where $\nu \geq \Delta$, i.e., the operating frequency being equal or larger than the zf gap, which is estimated as 145 GHz, corresponding to 4.8 cm^{-1}.

$Tp^{t\text{-}Bu,H}$Co(NCO). The 2-D field/frequency map (Figure 4b) shows the characteristic frequency value for which several inter-Kramers transitions branches converge in zero field at 350 GHz. This value corresponds to a zf gap, Δ, of about 11.7 cm^{-1}.

$Tp^{t\text{-}Bu,H}CoN_3$. This complex produced a particularly well-defined set of HFEPR resonances, although at the same time a strong torquing effect was observed (i.e., microcrystallite alignment with the large applied field), making it difficult to obtain perfect powder-pattern spectra.[28] The 2-D field/frequency map shown in Figure 4c is thus a summary of spectra obtained from several samples: some constrained in a pellet and some loose. It shows a zero-field frequency, where inter-Kramers turning points converge, of ca. 480 GHz. The value of Δ is thus about 16 cm^{-1}. A noteworthy feature of the spin Hamiltonian parameters for $Tp^{t\text{-}Bu,H}CoN_3$ (see Table 2) is the strong rhombicity of both the zfs tensor ($E/D \approx 0.2$) and, correspondingly, also the **g** matrix.

$Tp^{t\text{-}Bu,H}$CoCl. The 2-D field/frequency map shown in Figure 4d indicates the zero-field transition at the upper limit of the available frequency range, at ca. 650 GHz. The value of Δ is thus about 21.7 cm^{-1}. Figure 5 (lower part) shows how the sign of *D* was obtained from single-frequency spectra for this particular complex. In this case, the experimental spectrum was magnetically modulated, resulting in the conventional derivative shape. Note the presence of "pseudo-noise", particularly between 8 and 16 T, caused by a presence of discrete crystallites (despite grinding the sample) and the spread of resonances over a very large field range.[34] The experimental trace is in black, while the red (upper) trace represents a simulated spectrum obtained assuming a positive value of *D* and an ideal powder pattern. The blue (bottom) trace was simulated using a negative value of *D* of the same magnitude.

$Tp^{t\text{-}Bu,Me}$CoL Series. Each of the four complexes of this series produced a well-defined set of HFEPR resonances. Specific aspects of the spectral data for each complex are as follows.

$Tp^{t\text{-}Bu,Me}$Co(NCS). The 2-D field/frequency map (Figure S10a in the Supporting Information) shows the inter-Kramers turning points converging to zero field at about 165 GHz corresponding to $\Delta \approx 5.5$ cm^{-1}. Figure 5 (upper part) shows how the positive sign of *D* was obtained from single-frequency spectra for this particular complex. In this case, the experimental spectrum was optically modulated, resulting in an absorptive shape.

$Tp^{t\text{-}Bu,Me}$Co(NCO). The 2-D field/frequency map (Figure S10b in the Supporting Information) shows the inter-Kramers turning points converging to zero field at about 325 GHz corresponding to $\Delta \approx 11$ cm^{-1}.

$Tp^{t\text{-}Bu,Me}CoN_3$. The 2-D field/frequency map (Figure S10c in the Supporting Information) shows the inter-Kramers turning points converging to zero field at about 380 GHz corresponding to $\Delta \approx 12.5$ cm^{-1}. Note in Table 2 the unusually high values for g_x and g_y, 2.70 and 2.46, respectively, which were confirmed in repeated experiments.

$Tp^{t\text{-}Bu,Me}$CoCl. The 2-D field/frequency map (Figure S10d in the Supporting Information) shows the inter-Kramers turning points converging to zero field at the upper limit of the BWO sources, at ca. 680 GHz corresponding to $\Delta \approx 22.7$ cm^{-1}.

$Tp^{t\text{-}Bu,Tn}$CoL Series. The complexes $Tp^{t\text{-}Bu,Tn}$CoL (L = NCS^-, Cl^-) each produced a well-defined set of HFEPR; however, the complexes with L = NCO^-, N_3^- were difficult to handle, being of a very fluffy nature, and they also produced very poor quality HFEPR spectra. It was not possible to extract dependable values of spin Hamiltonian parameters from these spectra; therefore, these two complexes are left outside the current study. Specific aspects of the spectral data for the two complexes are as follows.

$Tp^{t\text{-}Bu,Tn}$Co(NCS). The 2-D field/frequency map (Figure S11a in the Supporting Information) shows the zero-field transition at ~207 GHz, which corresponds to $\Delta \approx 6.9$ cm^{-1}.

$Tp^{t\text{-}Bu,Tn}$CoCl. The 2-D field/frequency diagram (Figure S11b in the Supporting Information) shows that the zero-field frequency lies just above the current sources' limit, at about 720 GHz, yielding $\Delta \approx 24$ cm^{-1}.

Discussion

X-ray Crystallography. The crystal and molecular structures of numerous scorpionate complexes of Co(II) have been reported, with coordination numbers of 4, 5, and 6.[3] Of relevance here are four-coordinate complexes of general formula

(34) Krzystek, J.; Park, J.-H.; Meisel, M. W.; Hitchman, M. A.; Stratemeier, H.; Brunel, L.-C.; Telser, J. *Inorg. Chem.* **2002**, *41*, 4478–4487.

Table 1. Bond Distances (Å) and Angles (deg) Relevant to the Co(II) Coordination Sphere in $Tp^{R,R'}CoL$ Complexes

complex: R, R′; L[a]	d(Co−L)	d(Co−N(pz))[b]	θ(L−Co−N(pz))[c]	φ(N1(pz)−B−Co-N2(pz))[d]	τ(Co−E_{lig}−E_{int})[e]
3-*t*-Bu; Cl[f]	2.215	2.027, 2.044 *2 (2.038)	120.29, 122.23 *2 (121.58)	120.08 *2, 119.82 *2, 120.10 *2	
3-*t*-Bu, 5-Me; Cl[g]	2.208	2.023 2.036 *2 (2.028)	121.33 121.09 *2 (121.17)	119.02 *2, 119.73 *2, 121.23 *2	
3-*t*-Bu, 5-Me; Cl[h]	2.220	2.029 *3 (2.029)	121.51 *3 (121.51)	120.00 *6	
3-*t*-Bu, 5-Tn; Cl[h]	2.218	2.038, 2.040, 2.041 (2.040)	118.89, 121.41, 123.62 (121.31)	117.98, 119.04, 120.95, 121.36, 121.63, 119.04	
3-*i*-Pr, 4-*t*-Bu; Cl[i]	2.212	2.023, 2.040, 2.059 (2.041)	121.91, 120.93, 121.85 (121.56)	119.13, 120.88, 119.80, 118.40, 123.18, 118.61	
3-Ph, 5-Me; Cl[j]	2.200	2.026, 2.029, 2.045 (2.033)	124.97, 119.89, 120.99 (121.95)	116.96, 115.82, 122.96, 118.37, 124.63, 121.25	
3-*i*-Pr, 4-Br; Cl[k]	2.206	2.040 *2, 2.057 (2.046)	121.81 *2, 122.69 (122.10)	119.98 *2, 120.39 *2, 119.63 *2	
3-Ph_2CH; Cl[l]	2.208	1.995, 2.012, 2.029 (2.012)	120.57, 125.82, 120.87 (122.42)	118.87, 121.04, 120.13, 119.47, 120.44, 120.06	
3-*i*-Pr, 4-*t*-Bu; N_3[m]	1.911	2.011, 2.032, 2.044 (2.029)	126.81, 125.46, 117.81, (123.36)	120.03, 117.96, 120.01, 123.61, 118.49, 119.90	136.73
	1.907	2.023, 2.032, 2.033 (2.029)	118.06, 124.73, 121.70, (121.50)	118.22, 120.73, 120.13, 119.23, 121.83, 119.84	139.68
3-*t*-Bu; N_3[h]	1.919	2.035, 2.035, 2.032 (2.034)	117.90, 122.47, 124.39, (121.59)	120.35, 120.71, 120.94, 120.57, 118.08, 119.34	139.96
3-*t*-Bu, 5-Me; N_3[h]	1.920	2.030, 2.031, 2.039 (2.033)	119.48, 122.45, 122.77 (121.57) [116.03, 121.44, 126.93 (121.47)][v]	119.39, 119.94, 121.12, 121.22, 118.19, 120.13	148.58 [143.25][v]
3-Np; NCO[n]	1.892	2.006, 2.018, 2.019 (2.014)	120.21, 121.62, 125.88, (122.57)	118.59, 121.32, 119.56, 118.17, 122.21, 120.15	161.94
3-*t*-Bu; NCO[h]	1.906	2.024, 2.031, 2.037, (2.031)	119.76, 122.14, 122.77 (121.56)	120.09, 118.00, 119.57, 120.57, 121.00, 120.76	158.26
3-*t*-Bu, 5-Me; NCO[h]	1.916	2.011, 2.026, 2.031 (2.023)	118.57, 122.19, 122.73 (121.16)	119.84, 123.16, 120.20, 120.78, 116.26, 119.76	176.15
3-*t*-Bu; NCS[o]	1.910	2.013, 2.020, 2.025 (2.019)	119.29, 121.56, 123.15 (121.33)	119.69, 120.93, 118.04, 121.02, 120.14, 120.18	172.69
3-*t*-Bu, 5-Me; NCS[h]	1.915	2.003, 2.018, 2.023 (2.015)	120.24, 120.81, 121.57 (120.87)	116.99, 122.87, 114.28, 123.44, 117.27, 125.15	175.72
3-*t*-Bu, 5-Tn; NCS[h]	1.916	2.018, 2.019, 2.022 (2.021)	119.81, 122.11, 122.51 (121.48)	116.13, 126.37, 123.45, 115.02, 115.78, 123.24	166.76
3-*i*-Pr, 4-*t*-Bu; NCS[p]	1.897	1.983, 2.021, 2.082 (2.029)	118.60, 120.93, 123.83 (121.12)	123.32, 122.18, 119.38, 119.00, 118.08, 118.04	168.33
3-*i*-Pr, 4-Br; NCS[q]	1.925	2.016 *2, 2.039 (2.024)	119.03, 122.75 *2 (121.51)	120.33 *2, 120.10 *2, 119.57 *2	175.73
(3-*t*-Bu, $(3\text{-Ph})_2$); NCS[r]	1.907	2.023 *2, 2.023 (2.023)	120.10, 121.33 *2 (120.92)	120.45 *2, 119.79 *2, 119.76 *2	167.97
(3,5-*t*-Bu, $(3\text{-Ph})_2$); NCS[s]	1.917	2.017, 2.019, 2.030 (2.022)	117.71, 120.88, 125.66 (121.42)	118.59, 120.28, 121.82, 118.99, 121.41, 118.91	167.52
($3,5\text{-Me}_2$, (3-Ph,5-*i*-$Pr)_2$); NCS[t]	1.918	2.002, 2.012, 2.015 (2.010)	116.50, 120.60, 130.28 (122.46)	121.91, 115.61, 118.99, 123.58, 118.91, 121.01	168.17
(Ind-1, $(\text{Ind-2})_2$); NCS[u]	1.913	2.019, 2.020, 2.031 (2.023)	129.87, 97.02, 129.73 (118.87)	121.00, 120.76, 119.57, 120.57, 118.00, 120.09	167.11

[a] In addition to the listed complexes, there are several that are given in the CSD but do not provide 3-D coordinates (all reported by Trofimenko et al.[53]): R = 3-cHx (cHx = cyclohexyl), L = Cl, CSD code AHIRAK; R = c-Hx, R′ = 4-Br, L = Cl, CSD code AHIREO; R = 3-cHx, R′ = 4-Br, L = NCS, CSD code AHIRIS. Boldface type indicates complexes studied here by HFEPR. [b] The three Co−pyrazole-2N bond lengths (Å) and their average value (in parentheses). Note that certain of the molecules have a crystallographic symmetry plane making two lengths and corresponding angles equal (as indicated by *2). The mean of these Co−N bond distances for all complexes listed (counting both distinct $Tp^{i\text{-Pr},t\text{-Bu}}CoN_3$ molecules separately; see l below) is 2.027 Å with $\sigma = 0.016$ Å. [c] The three L−Co−N(pyrazole-N2) bond angles (deg) and their average value (in parentheses), which define the angle θ in the AOM analysis of the complexes studied here (see text). The mean of all of these angles is 121.61° (counting both distinct $Tp^{i\text{-Pr},t\text{-Bu}}CoN_3$ molecules separately) with $\sigma = 4.37°$. [d] The six N(pyrazole-N1)$_i$−B−Co−N(pyrazole-N2)$_j$ torsional angles (deg), where i and j are pyrazole ring identifiers, $i = 1-3$, $j = 1-3$, $j \neq i$, which define the angle ϕ in the AOM analysis of the complexes studied here (see text). These all average to 120.00°, as expected for this projection onto a circle. The standard deviation is 1.76°. The complex $Tp^{t\text{-Bu,Me}}CoCl$, as studied by us, has crystallographic 3-fold symmetry. [e] For L = polyatomic ligand (NCO, NCS, N_3), the tilt angle τ (deg) between Co and the coordinating (E_{lig} = N) and internal (E_{int} = C, N) atoms of the ligand. Use instead of the terminal atom of the ligand gives essentially the same values (within 0.5°), since the ligands are almost perfectly linear, with the exception of $Tp^{t\text{-Bu,Me}}CoN_3$, so that use of the terminal atom gives 148.81° [146.97°] (value for disordered ligand in brackets). [f] Reported by Gorrell and Parkin (CSD code SIBYUX).[17] The structure has a symmetry plane. [g] Reported by Ferrence and Beitelman (CSD code LEWJIH),[19] during the course of our own crystallographic studies. Note that the crystallographic symmetry in this case (symmetry plane) differs from that found here (3-fold symmetry). [h] This work (Tn = 2-thienyl). [i] Reported by Rheingold et al. (CSD code IKANEN).[54] [j] Reported by Uehara et al. (CSD code LUCHOG).[55] [k] Reported by Olson et al. (CSD code KIVKIJ).[56] [l] Reported by Rheingold et al. (CSD code ITAVUU).[57] [m] Reported by Rheingold et al. (CSD code IKANIR).[54] There are two crystallographically distinct molecules in the unit cell, and both sets of metrical parameters are given. [n] Reported by Calabrese and Trofimenko (Np = neopentyl; CSD code PARYIM).[58] [o] Reported by Trofimenko et al. (CSD code DOXBUN10).[18] [p] Reported by Rheingold et al. (CSD code IKANOX).[54] [q] Reported by Trofimenko et al. (CSD code JAJTOD).[59] [r] Reported by Łukasiewicz et al. (CSD code QAZCOJ);[60] this complex contains an unsymmetrically substituted scorpionate ligand. [s] Reported by Łukasiewicz et al. (CSD code QOKWUI);[61] this complex contains an unsymmetrically substituted scorpionate ligand. [t] Reported by Ruman et al. (CSD code OJEMOF);[62] this complex contains an unsymmetrically substituted scorpionate ligand. [u] Reported by Rheingold et al. (CSD code TASREK).[63] The ligand is derived from hydrotris(7-*tert*-butylindazol-2-yl)borate. However, a ligand rearrangement occurred so that the resulting complex is unsymmetrical: hydrogen(bis(7-*tert*-butylindazol-2-yl)(7-*tert*-butylindazol-1-yl)borato)(isothiocyanato)cobalt(II). [v] Two sets of values (one in brackets) are given due to disorder in the azido ligand.

$Tp^{R,R'}CoL$ (L = Cl^-, NCS^-, NCO^-, N_3^-). For our purposes here, the sole metric of interest is the inner coordination sphere of the Co(II) ion. Thus, the relevant factors are the metal−ligand bond lengths and angles, which are summarized in Table 1, and are important for the LFT analysis described below. More extensive geometric parameters are given in Table S2 (Supporting Information). An extensive discussion of these structures in the context of related Co(II) scorpionates is also given in the Supporting Information. The main point is that there is nothing structurally unusual about any of the complexes investigated here.

Electronic Absorption Spectroscopy: Band Assignments. Electronic absorption spectroscopic studies of (pseudo)tetrahedral Co(II) complexes go back many years, as summarized by Lever.[35] Of particular relevance here are spectra of bis(dihydrobis(1-pyrazolyl)borate)cobalt(II), $(Bp)_2Co$ (and its Zn(II) analogue, $(Bp)_2Zn$).[36] In this complex, there is an N4 donor set, as is the case with $Tp^{R,R'}CoL$ (L = NCS^-, NCO^-, N_3^-). Although the idealized local symmetry of $(Bp)_2Co$ is D_{2d} rather than C_{3v} in $Tp^{R,R'}CoL$, the electronic absorption spectra are very similar among all of these and we will begin by following the general assignments given for $(Bp)_2Co$. Bands at ~210 nm (>45 000 cm^{-1}) were observed for $(Bp)_2M$ (M = Co, Zn) and thus assigned to intraligand (pyrazole $\pi \rightarrow \pi^*$) transitions,[36] and we likewise assume that UV bands observed for $Tp^{R,R'}CoL$ have essentially no metal character. $(Bp)_2Co$ exhibits a well-resolved triplet in the visible region at 525−585 nm (19 000−17 000 cm^{-1}), which was assigned to the $^4A_2 \rightarrow {}^4T_1(P)$ transition (in T_d point group symmetry) and a doublet at 1070−1220 nm (9300−8200 cm^{-1}) in the near-IR, which was assigned to $^4A_2 \rightarrow {}^4T_1(F)$.[36] By careful comparison between spectra for the cobalt and zinc complexes in CH_2Cl_2 solution, a very weak band at 3120 nm (3200 cm^{-1}) was observed in the IR, which was assigned to $^4A_2 \rightarrow {}^4T_2$.[36] We did not have available complexes

(35) Lever, A. B. P. *Inorganic Electronic Spectroscopy*, 2nd ed.; Elsevier: Amsterdam, 1984.
(36) Jesson, J. P.; Trofimenko, S.; Eaton, D. R. *J. Am. Chem. Soc.* **1967**, *89*, 3148–3158.

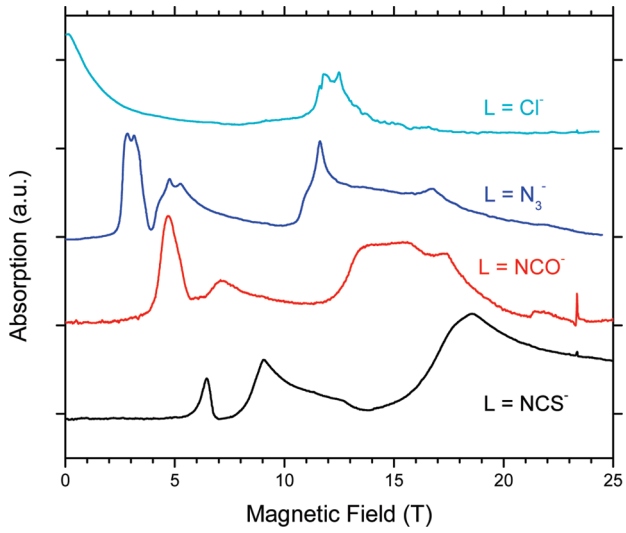

Figure 3. Assorted HFEPR spectra for the Tp$^{t\text{-Bu,H}}$CoL series at nearly the same frequency (655 GHz, except for L = N_3^- at 649 GHz) and T = 4.5 K using optical modulation (chopping the sub-THz wave beam at 250 Hz), with the resulting absorptive shape. The spectra were approximately normalized in amplitude. Note the near zero-field absorption in Tp$^{t\text{-Bu,H}}$CoCl at 655 GHz, which indicates the zf gap for this complex. The narrow line at 23.4 T is due to the DPPH marker.

of general formula Tp$^{R,R'}$ZnL, nor the free ligands, but comparison of IR spectra for Tp$^{R,R'}$CoL and CH_2Cl_2 solvent background gave no hint of a d−d band in this region. It should be noted that $(Bp)_2Co$ has effective D_{2d} point group symmetry, as opposed to TpCoL (C_{3v}); therefore, the analogy is not exact, although the transition $^4A_2 \rightarrow {}^4E(^4T_2)$ is x,y-dipole allowed in both point groups, and $^4A_2 \rightarrow {}^4B_2(^4T_2)$ in D_{2d} and $^4A_2 \rightarrow {}^4A_1(^4T_2)$ in C_{3v} are forbidden.

Tp$^{R,R'}$CoL complexes all exhibited strong, single bands at 1500−1650 nm (∼6000−6700 cm^{-1}) and at 910−960 nm (∼10 400−11 000 cm^{-1}) and a very intense band, often resolved into a triplet or quartet, at 540−650 nm (∼15 400−18 500 cm^{-1}). The major bands are given in Table 3, and a detailed listing is given in Table S3. The highest energy of the vis−near-IR bands clearly can be assigned to the $^4A_2 \rightarrow {}^4T_1(P)$ transition, by analogy of both its energy and line shape with those of $(Bp)_2Co$. The multiplet splitting within this band cannot be easily assigned, as it arises both from the symmetry being lower than T_d (T_1 splits into A_2 and E in both D_{2d} and C_{3v} symmetry) and from mixing in of doublet states via spin−orbit coupling. The wide variation in absorptivity among these complexes (see the Experimental Section) also suggests significant ligand character in these transitions. In particular, the very strong absorptivity of the dominant visible band centered at ∼600 nm for the azido and, to a lesser extent, for the thiocyanato complexes qualitatively suggests that the π-conjugated system of these ligands may be significantly mixed with the Co 3d orbitals, which greatly enhances the electronic transition dipole probability from that of a purer d−d transition, such as is the case for the chloro complexes.

The assignment of the bands at ∼930 nm (∼10 700 cm^{-1}) and the near-IR band at ∼1600 nm (∼6300 cm^{-1}) is considered next. More recently, Larrabee et al. performed a monumental MCD investigation of a wide range of Co(II) complexes, including Tp$^{t\text{-Bu,H}}$Co(NCS), which was studied as a poly(dimethylsiloxane) mull.[9] Their results are given in Table 2 and generally agree with those obtained here for Tp$^{t\text{-Bu,H}}$Co(NCS) in CCl_4 solution. Their band at ∼640 nm (15 700 cm^{-1}) is assigned to $^4A_2 \rightarrow {}^4T_1(P)$, as expected, and shows unresolved structure, as is also the case here. However, the bands at ∼940 nm (10 600 cm^{-1}) and at ∼1560 nm (6400 cm^{-1}) were both assigned to $^4A_2 \rightarrow {}^4T_1(F)$. The first of these assignments is in agreement with the earlier work of Jesson et al.;[36] however, in light of their work, we wished to confirm that the near-IR band is not due to $^4A_2 \rightarrow {}^4T_2(F)$.

Rather than going directly to an AOM analysis, which requires potentially a large number of parameters, we began with a simple crystal field model, which uses the parameters defined by Ballhausen:[37] Dq for the cubic (here tetrahedral) splitting and Ds for a trigonal distortion. It was possible to fit the above assignment quite successfully. However, to do so required an unreasonably small value for the Racah parameter, $B \approx 400-430$ cm^{-1}: i.e., only ∼40% of the free-ion value (variously reported as 989 cm^{-1} [31] or 1120 cm^{-1} [38]). This difficulty is a consequence of the large value of Dq that results from the assignment of the near-IR band to $^4A_2 \rightarrow {}^4T_2(F)$, so that B must be reduced to fit $^4A_2 \rightarrow {}^4T_1(P)$ in the region of 16 000 cm^{-1}. We conclude that the assignment of the electronic absorption bands, as shown in Table 3, due originally to Jesson et al.[36] and refined by Larrabee et al.[9] is definitive.

Electronic Absorption Spectroscopy: Ligand-Field Analysis. Among the many Tp$^{R,R'}$CoL complexes described herein, we begin the extraction of ligand-field parameters from electronic absorption spectra with Tp$^{t\text{-Bu,H}}$Co(NCS). This complex is chosen because it is one of two that have been investigated both by MCD, by Larrabee et al.,[9] and in this work by HFEPR, the other being Tp$^{t\text{-Bu,H}}$Co(NCO) (note that the ligand Tp$^{t\text{-Bu,H}}$ was referred to as L_1 by these workers[9]). A different series of Tp$^{R,R'}$CoL complexes (L = NCS^-, NCO^-, N_3^-) was studied by MCD, that with R = 3-Ph, and R′ = H (referred to as L_3[9]). This ligand is likely electronically similar to Tp$^{t\text{-Bu,H}}$ so that a direct comparison of effect of L is meaningful. As will be shown below, there are significant differences in the values obtained for zfs here by HFEPR and earlier by MCD, for analogous complexes or even the same complex. Lastly, Tp$^{R,R'}$CoL complexes were studied by MCD having L = Cl^-, NCS^-, R = 3-*i*-Pr, and R′ = 4-Br (this ligand was referred to as L_2).[9] Note that the bromo substituent is in the pyrazole ring 4- rather than 5-position and, further, may be significantly different electronically from the hydrocarbyl substituents studied here. Thus, comparison of results for Tp$^{3\text{-}i\text{-Pr},4\text{-Br}}$CoCl with the Tp$^{R,R'}$CoL series studied here might not be fully appropriate.

We use as a starting point the AOM parameters derived by Larrabee et al. for Tp$^{t\text{-Bu,H}}$Co(NCS), which successfully described their MCD spectra.[9] Following them, we did not include any π-bonding for either the thiocyanate or pyrazole nitrogen donors (and the latter were fixed at being equivalent). A good fit to the observed electronic transitions (see Table 3) was obtained with use of parameters only slightly modified from theirs (their values in parentheses; all values in cm^{-1}): ϵ_σ(N-pz) = 3750 (3700); ϵ_σ(N-CS) = 2520 (2670); B = 690 (736), $C = 4.3B$[31] (4.6B). More detailed listings of ligand-field fit parameters are given in Table S4.

Thus, as already shown by Larrabee et al.,[9] the AOM is quite successful at describing the electronic absorption spectra of a Tp$^{R,R'}$CoL complex: i.e., the quartet state energies. As seen in Table 2, and as discussed above (and in the Supporting

(37) Ballhausen, C. J. In *Introduction to Ligand Field Theory*; McGraw-Hill: New York, 1962; pp 99−103.
(38) Mabbs, F. E.; Collison, D. *Electron Paramagnetic Resonance of d Transition Metal Compounds*; Elsevier: Amsterdam, 1992.

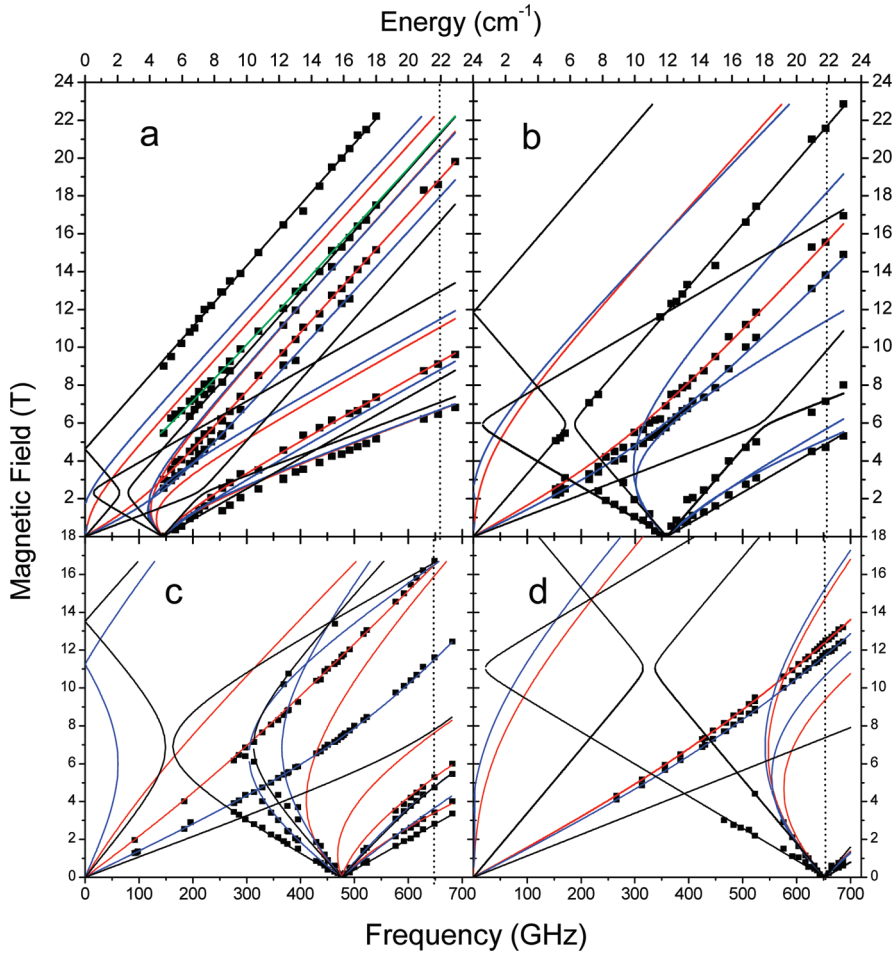

Figure 4. 2-D field/frequency (or quantum energy) maps of EPR turning points for the $Tp^{t\text{-}Bu,H}CoL$ series: (a) L = NCS^-; (b) L = NCO^-; (c) L = N_3^-; (d) L = Cl^-. The squares are experimental points, and the curves are simulated using best-fit spin Hamiltonian parameters as in Table 2. Red curves denote turning points with $B_0||x$, blue curves with $B_0||y$, and black curves with $B_0||z$, while the green curve in plot (a) is an off-axis turning point branch. The vertical broken lines indicate the frequency at which spectra in Figure 3 were collected. The data set corresponds to T = 4.5 K. Corresponding diagrams for the $Tp^{t\text{-}Bu,Me}CoL$ and $Tp^{t\text{-}Bu,Tn}CoL$ series are shown in Figures S10 and S11, respectively (Supporting Information).

Information), there would seem to be no structural basis for use of significantly different angular parameters for an AOM analysis of the other $Tp^{t\text{-}Bu,R'}CoL$ (L = pseudohalogen N-donor) complexes. The variation in θ and ϕ is on the order of tenths of degrees, which would be expected to have little effect. The variation in bond length could affect the bonding overlap parameters by r^{-5},[31,39] but here this is on the order of 0.01 Å, corresponding to ~3−4% changes in ϵ_σ, maximally ~100−150 cm^{-1}. Thus, little variation is expected for parameters of all $Tp^{t\text{-}Bu,R'}CoL$ (L = pseudohalogen N-donor) complexes. Indeed, Larrabee et al. determined for $Tp^{3\text{-}i\text{-}Pr,4\text{-}Br}Co(NCS)$ AOM parameters barely distinguishable from those for $Tp^{t\text{-}Bu,H}Co(NCS)$.[40] We therefore apply the same procedure to the remaining complexes, beginning with those also with $L = NCS^-$.

The electronic transitions for $Tp^{t\text{-}Bu,Me}Co(NCS)$ and $Tp^{t\text{-}Bu,Tn}Co(NCS)$ are only minimally different from those for $Tp^{t\text{-}Bu,H}Co(NCS)$ and the fit values that result using the crystallographically determined geometry provide a good fit to the observed transitions (see Table 3 and Table S3). Use of the procedure described above likewise provides a reasonable match to the electronic transitions for the two cyanato complexes (see Table 3). It is also possible to match successfully the electronic transitions for the two azido complexes using parameters that are quite similar to those of the other pseudohalogen complexes (see Table 3 and Table S4). The only hint as to the limits of this model is that the absorptivity of the azido complexes is unusually high at ~15 000 cm^{-1}. As noted above, the tilt angle of the azido ligand is much more pronounced (i.e., further from idealized 180°) than in the thiocyanato and cyanato complexes. It is possible that the azido ligand π-system is more closely coupled to the Co(II) unpaired electrons than in the other pseudohalogen complexes, which leads both to higher oscillator strength and a distorted structure.

Lastly, we come to the chloro complexes, in which L is no longer a period 2 atom. A structural feature of these complexes is that without a polyatomic L, with its tilt angle, higher symmetry is possible, which is the case for both $Tp^{t\text{-}Bu,H}CoCl$, with a symmetry plane, and for $Tp^{t\text{-}Bu,Me}CoCl$, with 3-fold symmetry (in our structure). A bonding feature of the chloro complexes is the greater possibility of π-donation from Cl lone pairs, although the similarity of the electronic absorption spectra with the pseudohalogen complexes suggests that this effect is not dominant. Thus, for all three of the chloro complexes, the electronic absorption spectra were successfully fitted with

(39) Gerloch, M.; Slade, R. C. In *Ligand-Field Parameters*; Cambridge University Press: Cambridge, U.K., 1973.

(40) Their fit parameters (in cm^{-1}) are as follows respectively for $Tp^{3\text{-}i\text{-}Pr,4\text{-}Br}Co(NCS)$ and $Tp^{t\text{-}Bu,\ H}Co(NCS)$: ϵ_σ(N-pyrazole) = 3720 vs 3700; ϵ_σ(N-CS) = 2500 vs 2670; B = 736 vs 740, ζ = 305 vs 383.9.

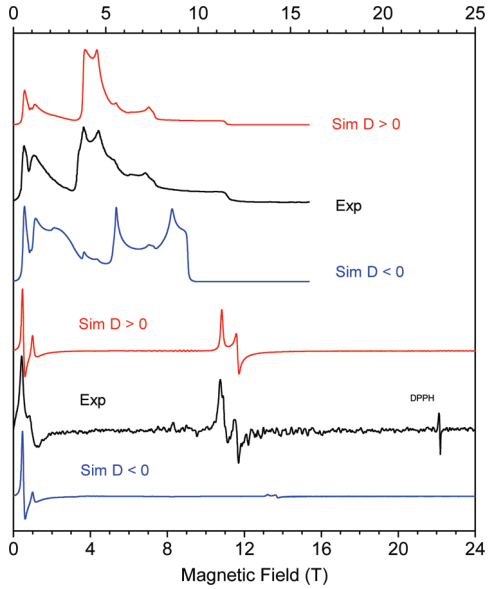

Figure 5. Examples of determining the sign of D from single-frequency spectra of Tp$^{t\text{-Bu,Me}}$Co(NCS) (upper set of three traces) and Tp$^{t\text{-Bu,H}}$CoCl (lower set of three traces). For both complexes, the chosen frequencies represent values near the zero-field gap. For Tp$^{t\text{-Bu,Me}}$Co(NCS), the experimental spectrum (upper black trace) was recorded at 168 GHz and 4.5 K using optical modulation, with the resulting absorptive shape. For Tp$^{t\text{-Bu,H}}$CoCl, the experimental spectrum (lower black trace) was recorded at 622 GHz and 4.5 K using magnetic modulation of the Zeeman field (1 kHz frequency, 2 mT amplitude), yielding a derivative shape. Red traces are spectra simulated using positive D values, while blue traces are spectra simulated using negative D values. The magnitudes of the simulation parameters for Tp$^{t\text{-Bu,Me}}$Co(NCS) are the same as in Table 2, while those for Tp$^{t\text{-Bu,H}}$CoCl are slightly different from those in Table 2: $|D| = 10.85$ cm^{-1}, $|E| = 0.23$ cm^{-1}, $g_x = g_y = 2.35$, $g_z = 2.05$. The narrow line in the lower experimental spectrum at 22.2 T is due to a DPPH marker.

parameters similar to those for the pseudohalogen complexes. Inclusion of cylindrical π-donation from the chloro ligand led to a marginally better fit, but this might be the consequence simply of having another adjustable parameter. The effect of the change in symmetry from 3-fold, to 2-fold, to none in going from R′ = H to Me to Tn had no perceptible effect on the fit parameters.

HFEPR Spectroscopy: Ligand-Field Analysis. The above ligand-field analysis of the electronic absorption spectra of the Tp$^{t\text{-Bu,R}'}$CoL is satisfying, and the similarity among the fit parameters would suggest that the zfs of these complexes would likewise be similar. Such a result is indeed suggested by the MCD analysis of Larrabee et al.,[9] in which the range of values determined for the zfs in Tp$^{R,R'}$CoL complexes is quite narrow: $3 \leq |\Delta| < 5$ cm^{-1}. Table S5 summarizes this "bottom line" obtained from either MCD or HFEPR studies (not included are values from other techniques[41,42]). In contrast, the range of zfs values determined by HFEPR is much larger: $4.8 \leq |\Delta| \leq 25.6$ cm^{-1} (see Table 2 and Table S5). Qualitatively, the zfs for the complexes with L = NCS$^-$ is the smallest, while for L = Cl$^-$, the period 3 ligand, Δ is much larger than for those with the pseudohalogen N-donors (period 2).

The ability of HFEPR to extract both D and E, not possible with MCD and exceedingly difficult with magnetometry,[34] allows a further qualitative comparison of each of these parameters among the complexes studied. As seen in Table 2, for the average values are as follows: L = NCS$^-$, $D \approx 3$ cm^{-1}; L = NCO$^-$, $D \approx 5.5$ cm^{-1}; L = N$_3^-$, $D \approx 7$ cm^{-1}, L = Cl$^-$, $D \approx 12$ cm^{-1}. However, such a generalization can be misleading since, for example, the D values for Tp$^{t\text{-Bu,H}}$Co(NCO) and Tp$^{t\text{-Bu,Me}}$CoN$_3$ are within 5% in magnitude, while the difference in D values between Tp$^{t\text{-Bu,H}}$Co(NCS) and Tp$^{t\text{-Bu,Tn}}$Co(NCS) is ~40%. The rhombicity of the complexes, given by E/D (see Table 2), ranges widely and no complex is truly axial: even Tp$^{t\text{-Bu,Me}}$CoCl with 3-fold crystallographic symmetry, which exhibited $E/D = 0.012$, the lowest such value, is clearly nonzero. Qualitative conclusions about zfs in these complexes thus are not easily drawn.

We then proceed with a quantitative analysis that combines the ligand-field parameters, on the basis of structural data for each complex that successfully fit the electronic absorption spectra, with the spin−orbit coupling interaction to yield calculated values for Δ. We begin with Tp$^{t\text{-Bu,Me}}$Co(NCS), a complex studied both by MCD and HFEPR. Inclusion of spin−orbit coupling with $\zeta = 420$ cm^{-1} gives an exact match to the value for Δ determined by HFEPR (see footnote to Table 2 and Table S4). Our calculation also reproduces the positive sign of D (i.e., $\langle S, M_S| = \langle {}^3/_2, \pm {}^1/_2|$ as the ground-state spin doublet), and the program Ligfield confirms the

Table 2. Spin Hamiltonian Parameters for the Three Series of Investigated Tp$^{t\text{-Bu,R}'}$CoL Complexes together with Experimental and Calculated Δ Values

complex[a]	D (cm^{-1})[b]	E (cm^{-1})[b]	E/D[c]	g_x	g_y	g_z
Tp$^{t\text{-Bu,H}}$Co(NCS)	+2.39(3)	+0.15(2)	0.063	2.27(1)	2.28(1)	2.21(1)
exptl Δ[d]	+4.81					
calcd Δ[e]	+4.81					
Tp$^{t\text{-Bu,Me}}$Co(NCS)	+2.69(1)	+0.15(1)	0.056	2.16(1)	2.18(1)	2.223(5)
exptl Δ[d]	+5.40					
calcd Δ[e]	−3.38					
Tp$^{t\text{-Bu,Tn}}$Co(NCS)	+3.34(1)	+0.49(1)	0.15	2.24(1)	2.27(1)	2.229(5)
exptl Δ[d]	+6.89					
calcd Δ[e]	+6.86					
Tp$^{t\text{-Bu,H}}$Co(NCO)	+5.98(2)	+0.17(2)	0.028	2.29(2)	2.43(2)	2.16(1)
exptl Δ[d]	+11.97					
calcd Δ[e]	+10.46					
Tp$^{t\text{-Bu,Me}}$Co(NCO)	+5.37(2)	+0.43(3)	0.080	2.16(2)	2.27(3)	2.222(5)
exptl Δ[d]	+10.84					
calcd Δ[e]	+9.80					
Tp$^{t\text{-Bu,H}}$CoN$_3$	+7.457(2)	+1.575(3)	0.21	2.48(2)	2.02(1)	2.31(2)
exptl Δ[d]	+15.88					
calcd Δ[e]	+11.24					
Tp$^{t\text{-Bu,Me}}$CoN$_3$	+6.32(2)	+0.48(4)	0.076	2.70(2)	2.46(2)	2.18(2)
exptl Δ[d]	+12.75					
calcd Δ[e]	+7.19					
Tp$^{t\text{-Bu,H}}$CoCl	+10.88(1)	+0.21(6)	0.019	2.34(2)	2.32(2)	2.11(2)
exptl Δ[d]	+21.77					
calcd Δ[e]	+17.71					
Tp$^{t\text{-Bu,Me}}$CoCl	+11.52(2)	+0.141(1)	0.012	2.35(1)	2.35(1)	2.24(1)
exptl Δ[d]	+23.04					
calcd Δ[e]	+14.62					
Tp$^{t\text{-Bu,Tn}}$CoCl	+12.72(4)	+0.78(2)	0.061	2.36(1)	2.20(1)	2.25(1)
exptl Δ[d]	+25.58					
calcd Δ[e]	+22.31					

[a] The complexes Tp$^{t\text{-Bu,Tn}}$Co(NCO) and Tp$^{t\text{-Bu,Tn}}$CoN$_3$ were also investigated by HFEPR but did not yield reliable spin Hamiltonian parameters (see text). [b] The sign of D is determined by experiment (see text); E is assigned the same sign by convention. [c] The maximum value for this rhombicity parameter is 0.33. [d] The D and E parameters are combined to give the zero-field gap (i.e., the zero-field splitting between the $\langle S, M_S| = \langle {}^3/_2, \pm {}^3/_2|$ and $\langle {}^3/_2, \pm {}^1/_2|$ manifolds) as follows: $\Delta = |2D\{1 + 3(E/D)^2\}^{1/2}|$. This Δ value is often all that can be estimated by other techniques (e.g., MCD; see Table S5) and is what is calculated here by LFT. [e] The LFT parameters used for the calculation (AOM parameters ϵ_σ(N-pz), ϵ_σ(L), ϵ_π(L); Racah parameters B, C; spin−orbit coupling constant ζ) are given in Table 2 and Table S4 (Supporting Information).

(41) Kuo, L. C.; Makinen, M. W. *J. Am. Chem. Soc.* **1985**, *107*, 5255–5261.
(42) Makinen, M. W.; Kuo, L. C.; Yim, M. B.; Wells, G. B.; Fukuyama, J. M.; Kim, J. E. *J. Am. Chem. Soc.* **1985**, *107*, 5245–5255.

Table 3. Visible−Near-IR Electronic Absorption Data for the Three Series of Investigated $Tp^{R,R'}CoL$ Complexes

	assignment in T_d				assignment in T_d		
complex	$^4A_2 \rightarrow {}^4T_1(P)$[a]	$^4A_2 \rightarrow {}^4T_1(F)$[b]	$^4A_2 \rightarrow {}^4T_2(F)$[c]	complex	$^4A_2 \rightarrow {}^4T_1(P)$[a]	$^4A_2 \rightarrow {}^4T_1(F)$[b]	$^4A_2 \rightarrow {}^4T_2(F)$[c]
$Tp^{t\text{-}Bu,H}Co(NCS)$				$Tp^{t\text{-}Bu,H}CoN_3$			not obsd
exptl[d]	15 150 (sh)	6 580	not obsd	exptl[d]	14 790	6 490	
	15 550				15 020 (sh)		
	15 900 (sh)	10 660			15 650 (sh)	10 820	
	16 810 (sh)				16 750 (sh)		
calcd[e]	15 050−15 240	6 400−6 580	2 660−3 090	calcd[k]	14 970−15 280	6 550−6 830	2 670−3 300
	15 970−16 310	10 670	5 190		15 990−16 430	10 960	5 360
$Tp^{t\text{-}Bu,H}Co(NCS)$[f]	15 700	6 400		$Tp^{t\text{-}Bu,Me}CoN_3$			
	16 800 (sh)	10 600		exptl[d]	15 000	6 500	not obsd
$Tp^{t\text{-}Bu,Me}Co(NCS)$					15 600 (sh)		
exptl[d]	14 800 (sh)	6 640	not obsd		16 650 (sh)	10 890	
	15 650			calcd[l]	14 960−15 210	6 550−6 820	2 680−3 200
		10 690			15 950−16 360	11 040	5 370
	16 760 (sh)			$Tp^{t\text{-}Bu,H}CoCl$			
calcd[g]	14 850−15 170	6 740−6 930	3 210−3 580	exptl[d]	15 080	6 060	not obsd
	16 000−16 360	10 770	5 280		15 800		
$Tp^{t\text{-}Bu,Tn}Co(NCS)$					16 640 (sh)	10 460	
exptl[d]	15 060 (sh)	6 670	not obsd	calcd[m]	15 030−15 270	6 140−6 320	2 050−2 620
	15 480				16 050−16 460	10 820	5 150
	15 920 (sh)	10 750		$Tp^{t\text{-}Bu,Me}CoCl$			
	16 750 (sh)			exptl[d]	15 150 (sh)	6 080	not obsd
calcd[h]	15 330−15 540	6 560−6 730	2 710−3 160		15 700		
	16 300−16 660	10 940	5 320		16 600 (sh)	10 500	
$Tp^{t\text{-}Bu,H}Co(NCO)$				calcd[n]	15 130−15 380	6 160−6 340	2 190−2 720
exptl[d]	15 020	6 450	not obsd		16 050−16 460	10 720	5 140
	15 480			$Tp^{t\text{-}Bu,Tn}CoCl$			
	16 260	11 010		exptl[d]	15 040	6 060	not obsd
	17 120				15 620		
calcd[i]	15 440−15 680	6 570−6 780	2 530−2 880		16 670 (sh)	10 620	
	16 340−16 760	11 120−11 210	5 440	calcd[o]	14 990−15 230	6 120−6 360	1 990−2 640
$Tp^{t\text{-}Bu,Me}Co(NCO)$					16 000−16 500	10 770−10 840	5 180
exptl[d]	15 510	6 460	not obsd	Bp_2Co[p]	17 100	8 200	3 200
	15 590				18 100	9 300	
	16 200	10 820			19 000		
	17 050 (sh)						
calcd[j]	15 570−15 800	6 580−6 790	2 660−3 220				
	16 430−16 880	10 980	5 380				

[a] In C_{3v} point group symmetry, the $^4T_1(^4P)$ excited state splits into $^4A_2$ (lower energy vis band) and ^4E (higher energy vis band); however, additional splitting can result from mixing in of lower energy doublet states, as shown by the calculations including spin−orbit coupling. [b] In C_{3v} point group symmetry, the $^4T_1(^4F)$ excited state splits into ^4E (lower energy, near-IR band) and $^4A_2$ (higher energy, vis/near-IR band). [c] In C_{3v} point group symmetry, the $^4T_2$ excited state splits into ^4E (mid-IR band; not observed here but seen for Bp_2Co;[36] see last entry of table) and $^4A_1$ (calculated near-IR band, but not observed, as this is a forbidden transition in C_{3v}). [d] This work, CCl_4 solution, room temperature; sh = shoulder. [e] Using the following parameters (values in cm^{-1}): ϵ_o(N-pz) = 3750, ϵ_o(N-CS) = 2520, all $\epsilon_\pi = 0$; $B = 690$, $C = 2970 = 4.3\ B$[31]; $\zeta = 420$. Spin−orbit coupling leads to numerous states; transitions with predominantly spin quartet character are indicated by range. These parameters yield the zfs, $\Delta = 4.81\ cm^{-1}$, as found by HFEPR (see Table 2 and Table S3). [f] Reported by Larrabee et al.,[9] diffuse reflectance of powders mixed with MgO, as in this work. Possible IR bands were not investigated. Their MCD spectra were of poly(dimethylsiloxane) mulls. [g] Using the following parameters (values in cm^{-1}): ϵ_o(N-pz) = 3790, ϵ_o(N-CS) = 3050, all $\epsilon_\pi = 0$; $B = 664$, $C = 4.3\ B$;[31] $\zeta = 455$; these yield: $\Delta = 3.38\ cm^{-1}$, lower than found by HFEPR (see Table 2 and Table S3). [h] Using the following parameters (values in cm^{-1}): ϵ_o(N-pz) = 3840, ϵ_o(N-CS) = 2585, all $\epsilon_\pi = 0$; $B = 703$, $C = 4.3\ B$[31]; $\zeta = 455$; these yield: $\Delta = 4.86\ cm^{-1}$, lower than found by HFEPR; these parameters but with $\zeta = 525\ cm^{-1}$ yields: $\Delta = 6.86\ cm^{-1}$, that found by HFEPR (see Table 2 and Table S3). [i] Using the following parameters (values in cm^{-1}): ϵ_o(N-pz) = 3900, ϵ_o(N-CO) = 2400, all $\epsilon_\pi = 0$; $B = 709$, $C = 4.3\ B$[31]; $\zeta = 530\ cm^{-1}$ yields: $\Delta = 10.22\ cm^{-1}$, slightly lower than that found by HFEPR (see Table 2 and Table S3). [j] Using the following parameters (values in cm^{-1}): ϵ_o(N-pz) = 3850, ϵ_o(N-CO) = 2530, all $\epsilon_\pi = 0$; $B = 715$, $C = 4.3\ B$[31]; $\zeta = 530\ cm^{-1}$ yields: $\Delta = 9.80\ cm^{-1}$, slightly lower than that found by HFEPR (see Table 2 and Table S3). [k] Using the following parameters (values in cm^{-1}): ϵ_o(N-pz) = 3840, ϵ_o(N−N_2) = 2670, all $\epsilon_\pi = 0$; $B = 680$, $C = 4.3\ B$[31]; $\zeta = 530\ cm^{-1}$ yields: $\Delta = 11.24\ cm^{-1}$, significantly lower than that found by HFEPR (see see Table 2 and Table S3). [l] Using the following parameters (values in cm^{-1}): ϵ_o(N-pz) = 3850, ϵ_o(N−N_2) = 2590, all $\epsilon_\pi = 0$; $B = 678$, $C = 4.3\ B$[31]; $\zeta = 530\ cm^{-1}$ yields: $\Delta = 7.19\ cm^{-1}$, significantly lower than that found by HFEPR (see Table 2 and Table S3). [m] Using the following parameters (values in cm^{-1}): ϵ_o(N-pz) = 3720, ϵ_π(N-pz) = 0, ϵ_o(Cl) = 2290, ϵ_π(Cl) = 440; $B = 712$, $C = 4.3\ B$[31]; $\zeta = 530\ cm^{-1}$ yields: $\Delta = 17.71\ cm^{-1}$, lower than that found by HFEPR (see Table 2 and Table S3). [n] Using the following parameters (values in cm^{-1}): ϵ_o(N-pz) = 3700, ϵ_π(N-pz) = 0, ϵ_o(Cl) = 2270, ϵ_π(Cl) = 275; $B = 713$, $C = 4.3\ B$[31]; $\zeta = 530\ cm^{-1}$ yields: $\Delta = 14.62\ cm^{-1}$, lower than that found by HFEPR (see Table 2 and Table S3). [o] Using the following parameters (values in cm^{-1}): ϵ_o(N-pz) = 3760, ϵ_π(N-pz) = 0, ϵ_o(Cl) = 2290, ϵ_π(Cl) = 500; $B = 711$, $C = 4.3\ B$[31]; $\zeta = 530\ cm^{-1}$ yields: $\Delta = 22.31\ cm^{-1}$, slightly lower than that found by HFEPR (see Table 2 and Table S3). [p] Reported by Jesson et al.,[36] in CH_2Cl_2 solution; Bp is dihydrobis(1-pyrazolyl)borate, which has D_{2d} symmetry.

expected $^4A_2$ ground state. We also calculated g values using these ligand-field parameters at high applied fields and obtained $g_x = 2.29$, $g_y = 2.28$, and $g_z = 2.26$, which are in the same ordering as found experimentally, although more isotropic, and give $g_{iso} = 2.28$, which is comparable to the experimental value, $g_{iso} = 2.26$.

The fit value for ζ is ~80% of the free-ion value (533 cm^{-1}[32]), while our fit value for B was 60−70% of the free-ion value.[31,38] In contrast, the values for B and ζ (383 cm^{-1}) determined by Larrabee et al.[9] are both ~70% of the free-ion value, but their value for the zfs is only $\Delta = 3.7\ cm^{-1}$. To match the ~30% larger value for Δ obtained from HFEPR, a larger value of ζ is

required. However, the difference in HFEPR-determined fit values for B and ζ relative to their free-ion values is not that serious, and thus the overall ligand-field analysis for $Tp^{t\text{-}Bu,Me}Co(NCS)$ would give one confidence in analyzing the remaining complexes, beginning with the others with L = NCS^-.

This confidence is not well justified. For $Tp^{t\text{-}Bu,Tn}Co(NCS)$, use of an even larger value for ζ (455 cm^{-1}, 85% of the free-ion value[32]) than employed above yields a Δ that is of correct (positive) sign but is too small in magnitude (4.9 vs 6.9 cm^{-1}). In order to obtain the observed zfs, a value for $\zeta = 525$ cm^{-1} (98% of the free-ion value[32]) is required. Likewise for $Tp^{t\text{-}Bu,Me}Co(NCS)$ use of a large value for ζ (455 cm^{-1}) yields a value for Δ that is too small in magnitude (3.4 vs 5.4 cm^{-1}), but in this case even the free-ion value does not achieve the experimental zfs, and the calculated value is of the wrong sign.

We then proceed to the cyanato series with some foreboding, given that although the MCD-derived values of Δ for $Tp^{t\text{-}Bu,H}Co(NCO)$ and for $Tp^{3\text{-}Ph}Co(NCO)$ (see Table S5) are quite close to those for their thiocyanato analogues, we have found by HFEPR that these complexes exhibit relatively larger zfs. The calculated value for Δ (6.01 cm^{-1}) resulting from the value of ζ used for $Tp^{t\text{-}Bu,H}Co(NCO)$ (420 cm^{-1}) is much smaller than that observed (11.97 cm^{-1}), but it is larger than that for the thiocyanato complexes, showing the correct trend. Use of essentially the free-ion value for ζ (530 cm^{-1}) significantly increases the zfs to 10.46 cm^{-1}, nearly the experimental value, and the positive sign also obtains. The situation is almost the same with $Tp^{t\text{-}Bu,Me}Co(NCO)$: use of $\zeta = 420$ cm^{-1} affords $\Delta = 5.80$ cm^{-1}, which, while smaller than the experimental value, is also smaller than that calculated for $Tp^{t\text{-}Bu,H}Co(NCO)$, as is the case experimentally, and so the relative ordering is correct. The positive sign of D is also reproduced. As before, use of the free-ion ζ value gives $\Delta = 9.80$ cm^{-1}, which approaches the experimental value.

We then turn to the azido complexes, the last of the L = pseudohalogen complexes to be investigated. The zfs for $Tp^{t\text{-}Bu,H}CoN_3$ is the largest among this group, $\Delta = +15.88$ cm^{-1}, and it would seem unlikely that such a value could be obtained from the methods used here. Use of $\zeta = 420$ cm^{-1} affords $\Delta = 7.13$ cm^{-1}, which is larger than that for the other complexes, as is the case experimentally; thus, this relative ordering is again correct. A positive sign of D is also reproduced. Use of the free-ion value ζ gives $\Delta = 11.24$ cm^{-1}, which approaches the experimental value (i.e., ~70% thereof). It is clearly impossible using the current model to achieve a zfs of nearly 16 cm^{-1}. A similar situation obtains for $Tp^{t\text{-}Bu,Me}CoN_3$; use of $\zeta = 420$ cm^{-1} yields only $\Delta = 4.20$ cm^{-1}, with a positive sign of D. Use of the free-ion value ζ gives $\Delta = 7.19$ cm^{-1}, which is <60% of the experimental value.

Finally, we come to the chloro complexes, in which L is no longer a period 2 atom. The possible contribution of spin−orbit coupling from this ligand would be greater than that for lighter atoms, as described elsewhere.[43,44] Unfortunately, no identical complex was studied by Larrabee et al.,[9] although they reported for $Tp^{3\text{-}i\text{-}Pr,4\text{-}Br}CoCl$, $\Delta = 4.8$ cm^{-1}, in line with the other $Tp^{R,R'}CoL$ complexes. HFEPR, however, provides zfs that is far out of range of the pseudohalogen complexes, $\Delta > 20$ cm^{-1}. Inclusion of spin−orbit coupling using the AOM parameters both without and with Cl π-donation led to values of Δ that were significantly larger than those calculated for the complexes with pseudohalogen ligands but still much smaller than experiment. Inclusion of π-bonding led to slightly larger values for Δ than without; therefore the results presented in Table 2 and Table S4 include this effect.

Clearly, a simple ligand-field model using only a d^7 basis set has serious limitations, significantly underestimating the zfs. However, this model is not without benefits, not only in analyzing the electronic absorption spectra but also in the zfs, given that the underestimation of zfs ranges from 0 to 40%, not by an order of magnitude or more. Furthermore, in almost all cases the sign of D is correctly predicted and the relative ordering of zfs magnitude among similar complexes is also correctly given. Far more sophisticated computational methods would be required to reproduce the experimental spin Hamiltonian parameters, such as the DFT programs employed by Neese and co-workers, which include intramolecular spin−spin coupling,[45] as well as the spin−orbit contribution of the ligands.

Another point is the discrepancy between the values for Δ determined by MCD versus those from HFEPR (see Table S5). In contrast, we have found, admittedly in a study involving only a single HS Co(II) complex, good agreement between these two techniques.[13] We can only speculate as to two reasons for this discrepancy. One is an experimental one, namely that use of multiple wavelengths is necessary to obtain a VTVH-MCD data set that is sufficient to provide reliable data for extraction of spin Hamiltonian parameters,[13] while it appears that only a single wavelength (595 nm) was employed for the scorpionate complexes studied by VTVH-MCD.[9] Given the enormous number of complexes in that study, one can hardly fault the choice made at that time. Another is a theoretical/computational one: namely that more sophisticated methods of analysis of MCD spectra, such as those developed by Solomon and co-workers,[46−48] and reported subsequent to the work of Larrabee et al.,[9] might prove more successful in this analysis. Indeed, such methods are now being used by Larrabee and co-workers in their recent MCD work on dinuclear Co(II) systems.[49−52]

A final point is a qualitative one but is perhaps the most important and has already been emphasized by Larrabee et al.[9] Four-coordinate Co(II) scorpionate complexes that superficially seem to be almost identical, e.g., by the substitution of H by Me on a ligand pyrazole, can be electronically very different as revealed by HFEPR, a technique superbly sensitive in extracting spin Hamiltonian parameters with high precision. Thus, Co(II)-substituted Zn enzymes might likewise exhibit a wide range of zfs values, resulting from very subtle structural changes in their amino acid (e.g., tris histidine) coordination geometry. The effect of the ancillary ligand, L, is harder to relate to Zn proteins. All of the pseudohalogen ligands used are

(43) Desrochers, P. J.; Telser, J.; Zvyagin, S. A.; Ozarowski, A.; Krzystek, J.; Vicic, D. A. *Inorg. Chem.* **2006**, *45*, 8930–8941.
(44) Mossin, S.; Weihe, H.; Barra, A.-L. *J. Am. Chem. Soc.* **2002**, *124*, 8764–8765.
(45) Ganyushin, D.; Neese, F. *J. Chem. Phys.* **2006**, *125*, 024103.
(46) Neese, F.; Solomon, E. I. *Inorg. Chem.* **1999**, *38*, 1847–1865.
(47) Wei, P.-p.; Skulan, A. J.; Mitić, N.; Yang, Y.-S.; Saleh, L.; Bollinger, J. M.; Solomon, E. I. *J. Am. Chem. Soc.* **2004**, *126*, 3777–3788.
(48) Wei, P.-p.; Tomter, A. B.; Røhr, Å. K.; Andersson, K. K.; Solomon, E. I. *Biochemistry* **2006**, *45*, 14043–14051.
(49) Larrabee, J. A.; Johnson, W. R.; Volwiler, A. S. *Inorg. Chem.* **2009**, *48*, 8822−8829.
(50) Johansson, F. B.; Bond, A. D.; Nielsen, U. G.; Moubaraki, B.; Murray, K. S.; Berry, K. J.; Larrabee, J. A.; McKenzie, C. J. *Inorg. Chem.* **2008**, *47*, 5079–5092.
(51) Larrabee, J. A.; Chyun, S.-A.; Volwiler, A. S. *Inorg. Chem.* **2008**, *47*, 10499–10508.
(52) Larrabee, J. A.; Leung, C. H.; Moore, R. L.; Thamrong-nawasawat, T.; Wessler, B. S. H. *J. Am. Chem. Soc.* **2004**, *126*, 12316–12324.

potentially π-interacting, but the LFT analysis did not reveal any π-interaction with Co(II). Biological ligands such as Glu, Asp (carboxylato), Cys (thiolato), and aqua/hydroxo are all potential π-donors, and their effect on electronic structure may be as profound as the variation seen here among pseudohalogen ligands. By analogy with the results reported here for L = Cl^-, a period 3 atom with spin−orbit coupling correspondingly larger than that for period 2 atoms, metalloenzymes with sulfur-donor ligands (the biologically relevant period 3 donor atom) could exhibit very large zfs, despite being structurally very similar to those with only N,O-donor amino acid ligands. The final message is that the relation of spin Hamiltonian parameters to coordination chemistry in four-coordinate Co(II) is far from being fully understood.

Conclusions

We have reported the crystal structures, electronic absorption spectra, and HFEPR spectra for a series of four-coordinate HS Co(II) scorpionate complexes, of general formula $Tp^{t\text{-}Bu,R'}CoL$. HFEPR is very well suited to extraction of intrinsic $S = {}^3/_2$ spin Hamiltonian parameters of these complexes. In contrast, there might be difficulties related to analogous analysis of MCD data. The complexes are very similar in terms of their molecular structure and electronic absorption spectra, and a ligand-field analysis of their electronic structure using these data is reasonably successful. However, the calculated zfs is consistently smaller than that found experimentally and subtle differences in ligand geometry can have large effects on these parameters. The key message from this model compound study is that great care must be taken in correlating spin Hamiltonian parameters with details of coordination geometry and ligand type. Spectroscopic data for Co(II)-substituted Zn enzymes are of potentially great utility, but their analysis must employ very sophisticated computational methods, not "rules of thumb".

Acknowledgment. HFEPR studies were supported by the National High Magnetic Field Laboratory, which is funded by the NSF through Cooperative Agreement DMR 0654118, the State of Florida, and the DOE. J.K. and J.T. were awarded an NHMFL UCGP grant (No. 5062). The 25 T resistive magnet was funded by the W. M. Keck Foundation. Funding from the Goldenberg Foundation supported purchase of a UV−vis−near-IR spectrophotometer at Roosevelt University. We also thank the Department of Chemistry, University of Iowa, Working Weekends Program, for support of the crystallographic studies and Dr. J. Bendix, Ørsted Institute, Copenhagen, Denmark, for use of the program Ligfield and assistance with development of the program DDN. We thank Prof. Thomas C. Brunold and Dr. Matthew Liptak, University of Wisconsin, Madison, for helpful comments. Finally, all the complexes used in this study were kindly delivered by Dr. Swiatoslaw (Jerry) Trofimenko, who passed away on Feb 26, 2007, and we dedicate this paper to his memory.

Supporting Information Available: Text giving a detailed discussion of the structural data for the eight complexes crystallographically characterized herein, $Tp^{t\text{-}Bu,R'}CoL$ (R′ = H, L = NCO^-, N_3^-; R′ = Me, L = Cl^-, NCS^-, NCO^-, N_3^-; R′ = Tn, L = Cl^-, NCS^-), in the context of other $Tp^{R,R'}CoL$ complexes, tables giving crystallographic data collection information and complete listings of bond distances, angles, and atomic anisotropic thermal parameters for the eight crystallographically characterized $Tp^{t\text{-}Bu,R'}CoL$ complexes, complete UV−vis−near-IR data, complete LFT parameters, and a comparison of MCD and HFEPR results., CIF files giving crystallographic data for these eight compounds, and figures showing the structures of these eight compounds, unscaled UV−vis−near-IR spectra, and 2-D field/frequency maps of HFEPR turning points for the $Tp^{t\text{-}Bu,Me}CoL$ and $Tp^{t\text{-}Bu,Tn}CoL$ series of complexes. This material is available free of charge via the Internet at http://pubs.acs.org.

JA910766W

(53) Trofimenko, S.; Rheingold, A. L.; Liable Sands, L. M. *Inorg. Chem.* **2002**, *41*, 1889–1896.
(54) Rheingold, A. L.; Liable-Sands, L. M.; Golan, J. A.; Trofimenko, S. *Eur. J. Inorg. Chem.* **2003**, 2767–2773.
(55) Uehara, K.; Hikichi, S.; Akita, M. *J. Chem. Soc., Dalton Trans.* **2002**, 3529–3538.
(56) Olson, M. D.; Rettig, S. J.; Storr, A.; Trotter, J.; Trofimenko, S. *Acta Crystallogr.* **1991**, *C47*, 1543–1544.
(57) Rheingold, A. L.; Liable-Sands, L. M.; Golen, J. A.; Yap, G. P. A.; Trofimenko, S. *Dalton Trans.* **2004**, 598–604.
(58) Calabrese, J. C.; Trofimenko, S. *Inorg. Chem.* **1992**, *31*, 4810–4814.
(59) Trofimenko, S.; Calabrese, J. C.; Domaille, P. J.; Thompson, J. S. *Inorg. Chem.* **1989**, *28*, 1091–1101.
(60) Łukasiewicz, M.; Ciunik, Z.; Wołowiec, S. *Polyhedron* **2000**, *19*, 2119–2125.
(61) Łukasiewicz, M.; Ciunik, Z.; Ruman, T.; Skora, M.; Wołowiec, S. *Polyhedron* **2001**, *20*, 237–244.
(62) Ruman, T.; Ciunik, Z.; Wołowiec, S. *Eur. J. Inorg. Chem.* **2003**, 2475–2485.
(63) Rheingold, A. L.; Liable-Sands, L. M.; Yap, G. P. A.; Trofimenko, S. *Chem. Commun.* **1996**, 1233–1234.